8-2016

Investigation of the Interaction of Dimeric Ruthenium Complexes with Cytochrome b5

Christopher Dain Rupar
University of Arkansas, Fayetteville

Investigation of the Interaction of Dimeric Ruthenium
Complexes with Cytochrome b_5

A dissertation submitted in partial fulfillment
of the requirements for the degree of
Doctor of Philosophy in Chemistry

by

Christopher Dain Rupar
Missouri Southern University
Bachelor of Science in Chemistry, 2000

August 2016

This dissertation is approved for recommendation to the Graduate Council

_____

Dr. Bill Durham
Dissertation Director

_____   _____

Dr. Francis Millett   Dr. Roger E. Koeppe, II
Committee Member   Committee Member

_____

Dr. Wesley Stites
Committee Member

Abstract

Photoreactive complexes to study the kinetics of electron transfer of proteins have been in use for a long time. It has always been speculated that complexes bind near the heme or the electron transfer reaction would not occur. But it is unkown exactly how the complex interacts with the protein. The structural, thermodynamic, and kinetic properties of rat liver microsomal cytochrome b_5 were investigated when bound to ruthenium dimer complexes. Heteronuclear Single Quantum Coherence studies support a dynamic binding model of a dimer Ru complex bound near the protein's heme involving residues H39, E44, G42, V61, G62, and H63. The enthalpy of binding ΔH was found to be unfavorable: +200 cal/mol, despite a very favorable equilibrium dissociation constant K_d was found to be 40 μM indicating an entropically controlled process. These insights will help with the design of future photoreactive complexes for the study of electron transfer reactions in metalloproteins.

Acknowledgements

      I would like to thank my wife whose never ending support and encouragement has allowed me to fulfill my dreams. I would like to thank my mother who always taught me to be the best I can be. I want to thank my advisor, Dr. Bill Durham, who never gave up on me, and my distinguished committee members, Dr. Frank Millett, Dr. Roger Koeppe, and Dr. Wesley Stites, for their advice and guidance. I want to thank the mentors that have helped me in my journey, Dr. Andy Williams, Dr. Lois Geren, and Dr. Srinvas Jianthi. And I would like to thank the friends I've made through the years as a graduate student, Dr. Jeff Havens, Dr. Jeremy Durchman, Dr. Randy Espinol, and Dr. Roland Njabon. Special thanks to Marilyn Davis for her work with N enriched proteins and Dr. Latisha Puckett for her work with ruthenium dimer complexes.

Dedication

This dissertation is dedicated to my father, who always instilled in me a passion for science.

Table of Contents

List of Tables and Figures

Chapter 1 -- Introduction

1.1 The Electron Transport Chain

All organisms require energy to drive the biochemical processes that are necessary for life

functions. This is accomplished, in part, by a series of electron transfer reactions between

hemeproteins bound to the mitochondrial membrane. These metalloproteins make up an electron

transport chain which is part of the metabolic pathway known as oxidative phosphorylation. The

free energy from electrons moving through the system is utilized to create a proton gradient

across the mitochondrial or chloroplast membrane. This buildup of protons creates concentration

imbalance. The free energy from restoring this imbalance is used to convert adenosine

diphosphate, ADP, into adenosine triphosphate, ATP (respiration) (Cordes et al., 2009). ATP is

used to power the various reactions needed to grow, reproduce, and maintain life. Figure 1-1

depicts a representation of the typical electron transfer reactions involved in respiration (Raven

et al., 1986). Moreover, electron transfer between proteins is a fundamental step for many other

metabolic processes (Cordes et al., 2009).

In respiration, the production of energy typically begins with the metabolism of glucose in

glycolysis and the citric acid cycle. During these processes, the molecules nicotinamide adenine

dinucleotide (NADH) and flavin adenine dinucleotide ($FADH_2$) are produced in a reduced form.

The first mitochondrial protein in the electron transport chain is known as NADH-Q

oxidoreductase, or complex I.   Complex I oxidizes NADH and transfers two electrons to

through several iron-sulfur clusters to reduce lipid soluble coenzyme Q, also called Q or

Figure 1-1: Representation of the electron transfer reactions involved in respiration.
Raven, P. H., and G. B. Johnson. 1986. Biology. 2nd ed. St. Louis, Mo.: Times Mirror/Mosby College.

NADH
DEHYDROGENASE
COMPLEX

CYTOCHROME *b-c*
COMPLEX

CYTOCHROME OXIDASE
COMPLEX

H⁺

H⁺   H⁺

Cyt. c

NADH
+ H⁺

H⁺

NAD⁺

$2H^+ + ½O_2$

H⁺

MATRIX

ATP

H₂O

ADP

HIGHER H⁺
CONCENTRATION
IN OUTER
COMPARTMENT

ATP

H⁺

ATP CHANNEL

RESPIRATORY
ASSEMBLY

3
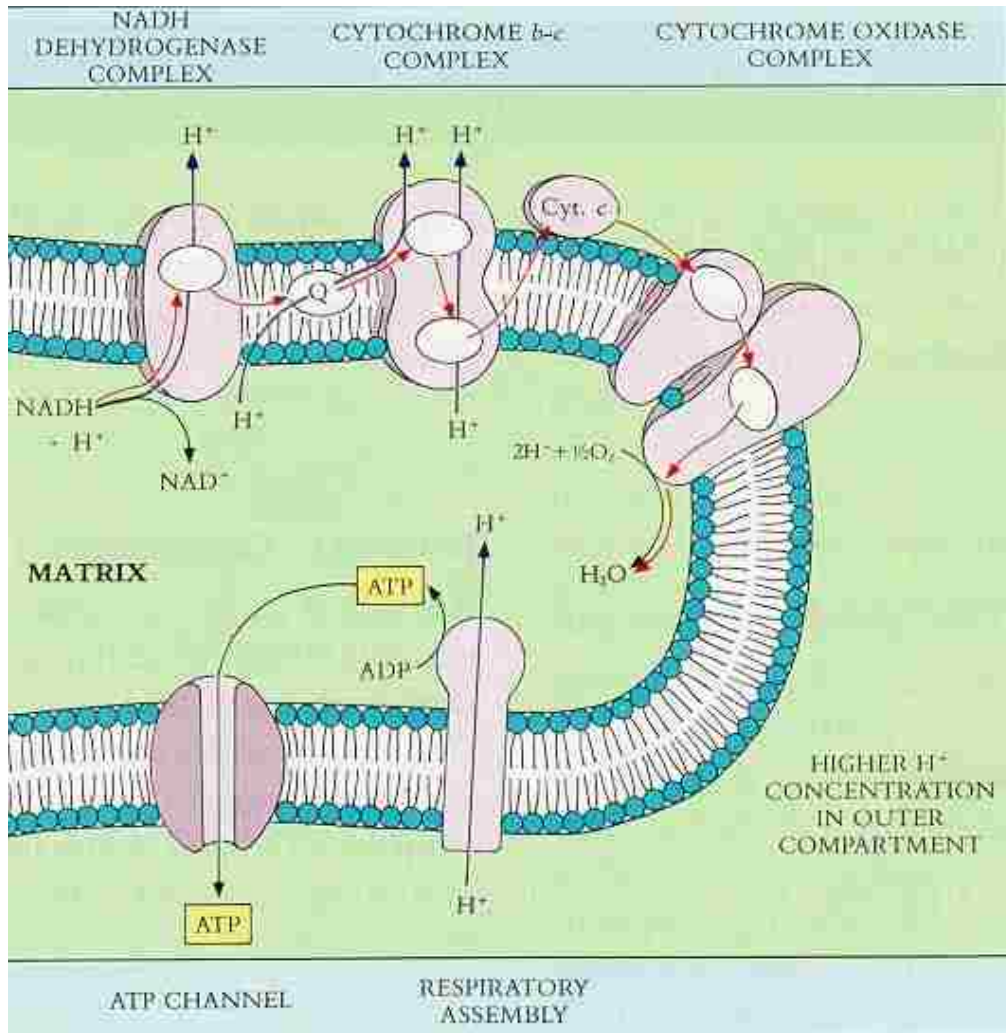
ubiquinone, inside the membrane. During this process, four protons are pumped from the mitochondrial matrix to the intermembrane space.

Succinate-Q oxidoreductase, also known as complex II, reduces succinate to fumarate as part of the Krebs cycle. Electrons are transferred through an $FADH_2$ prosthetic group as well as a series of iron-sulfur clusters to reduce coenzyme Q to QH_2, or ubiquinol. No protons are translocated as a result of these electron transfers. Complex II contains an iron heme group that does not play a role in the reduction of Q, but may be involved in reducing the production of reactive oxygen species (Yankovskaya et al., 2003).

Complex III is also called Q-cytochrome c oxidoreductase or cytochrome bc_1, and only functions as a dimer. Complex III transfers electrons from QH_2 through an iron-sulfur cluster and three cytochromes: one cytochrome c_1 and two b cytochromes (Iwata et al., 1998). One electron is used to reduce a cytochrome c molecule that is electrostatically bound. The other goes through a Q-cycle to partially reduce a ubiquinone molecule. After two molecules of QH_2 have been oxidized, two molecules of cytochrome c have been reduced and one ubiquinone has been reduced back to an ubiquinol, which enters back into the QH_2 pool (Berry et al., 2000). As a result, four protons are pumped to the inner membrane space.

Reduced cytochrome c then binds electrostatically to complex IV, cytochrome c oxidase. Electrons enter cytochrome oxidase from cytochrome c through a copper redox center Cu_A. The electrons then travel through a heme a, to a binuclear center with a heme a_3 and Cu_B. From there, the electrons reduce bound molecular oxygen, which is the final electron acceptor in the chain. It takes four electrons to reduce molecular oxygen to two waters, so the cycle involves the binding of four cytochrome c molecules. In the process, four protons are pumped across the inner mitochondrial membrane.

1.2 The Study of Biological Electron Transfer

Studies of the structure these proteins (Argos et al., 1975; Iwata et al., 1998; Berry et al., 2000; Grigorieff, 1998; Sun et al., 2005) initiated a wide variety of investigations into the nature of electron transfer reactions. An important aspect of understanding these reactions is measuring the rate of electron transfer. Determining the kinetics of electron transfer while varying the conditions such as temperature, ionic strength, viscosity, and mutated residues, gives important insight to the nature of biological electron transfer (Durham et al. 1997). Important concepts include how electrons are transferred efficiently between redox centers, how electron transfer is coupled to charge gradients and the production of energy, recognition between natural electron transfer partners, and the regulation of the flow of electrons *in vivo* (Durham et al. 1997).

An electron-transfer reaction that does not involve breaking or making of bonds is classified as an , outer-sphere electron transfer reaction (Davidson, 2000). This classification was originally developed to describe simple inorganic reactions and on loosely holds for the reactions of most metalloproteins (Gray et al., 2003). In these reactions the ligands immediately surrounding the metals remain intact during the redox process and thus the criteria is met. However, the process of creating the proton gradient does involve bond changes although remove from the metal center.

Many biological electron transfer reactions actually occur faster than 10^3 s^{-1}, (27). This means that the method of monitoring the reaction must be faster than the reaction itself, or the determined kinetics will be limited by the recording device. One method commonly used to investigate fast reactions is stopped-flow. This method works by rapid mixing two different

5

solutions of redox reactive biological species though injection. However, the method is limited by mixing time, which precludes this method for any reaction that occurs faster than a few milliseconds.

Pulse radiolysis is a technique that can be applied to very fast reactions. This method utilizes a rapid burst of high energy-electrons to generate reactive species in solution. (Isied et al., 1984). This method, however, is non-specific and many reactive species are often generated. A variety of reagents are typically added to the solutions of interest in order to scavenge for unwanted reactants. Despite this difficulty some early work with metalloproteins was performed successfully with this technique.

Flash photolysis is another rapid kinetic method with an early development history similar to pulse radiolysis. Development of turn-key lasers, fast transient recorders and personal computers made laser flash photolysis one of the primary tools for the study of all aspects of electron transfer. This technique uses a short laser pulse to create the reactive species instead of a high energy electron pulse. The basic instrumental configuration is shown in Figure 1-2. Some molecules are naturally photoreactive and the photoreaction is used to create the reactive species. In other cases a photoreactive molecule is added and various reaction schemes are used to create the appropriate reactants. Reactions are typically followed spectrophotometrically.

Metalloproteins in general are not photoreactive and without some modification are not suitable for the flash photolysis experiment. One modification is substitution of the metal to produce a photoreactive metal center. A few researchers have substituted a zinc atom in place of an iron in a heme. When the zinc-substituted heme is hit with a laser flash, its excited state lifetime is sufficient to transfer an electron to an acceptor protein (Peterson-Kennedy et al., 30).

Figure 1-2: Typical setup of a laser flash photolysis experiment. *Havens, J. (2010) "Ruthenium flash initiated studies of electron transfer between cytochrome c and the b hemes of cytochrome b_5 and sulfite oxidase, and the electron transfer within cytochrome bc1" Dissertation, University of Arkansas, Fayetteville, AR*

Tungsten lamp

Laser

⬭ Lens

▭ Filter

sample holder

Prism

monochromator

Photomultiplier Tube Detector

Oscilloscope

S1 Fittings software
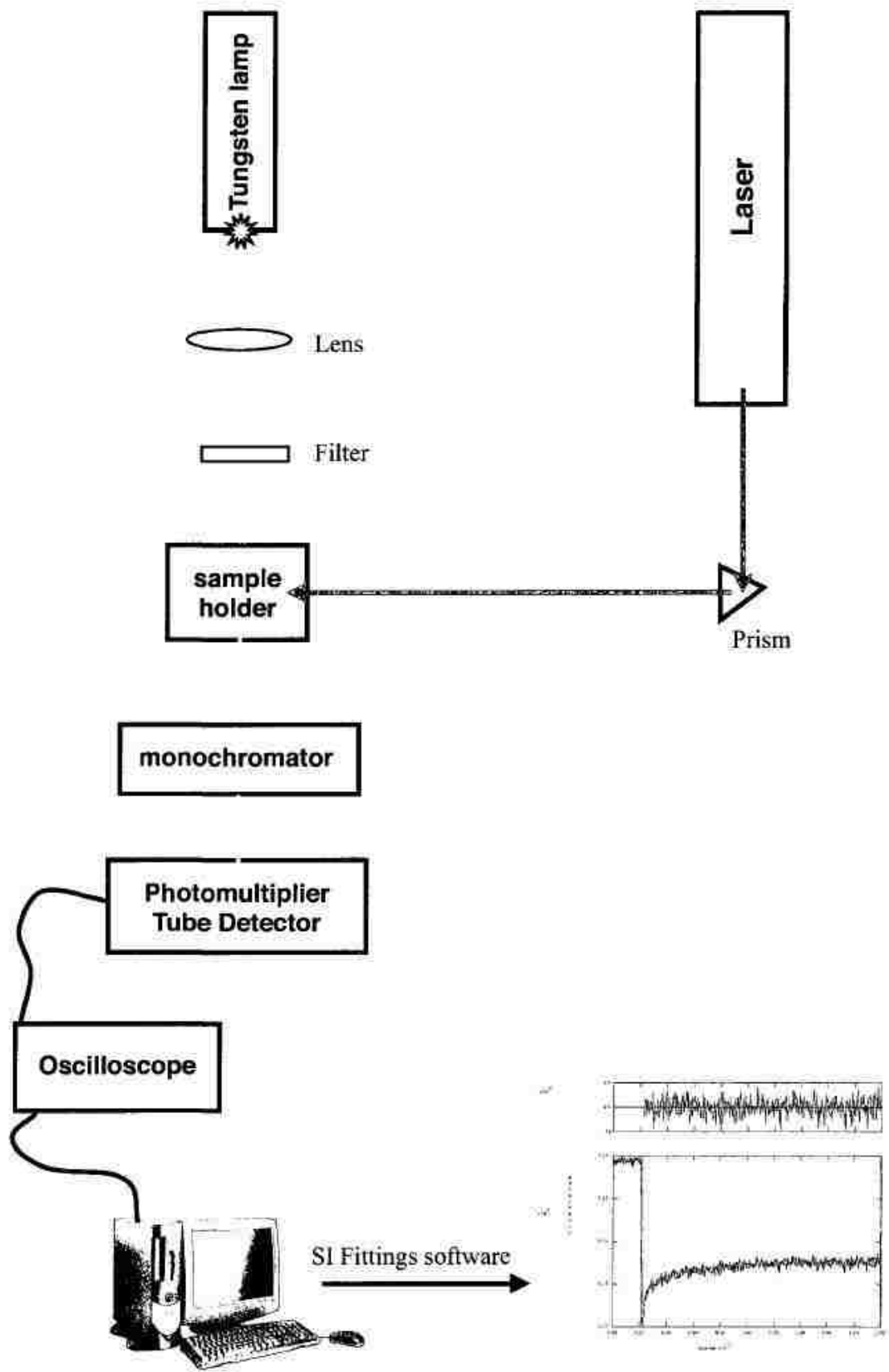
While the substitution of a zinc atom causes little structural change within the protein, it is not native and some of its properties such as redox potential are altered.

Nocera et al. (1984) and Isied et al. (1982) were able to covalently link a $[Ru(NH_3)_5]^{2+}$ complex to a surface histidine of cytochrome c. Techniques like the previously described pulse radiolysis or zinc-heme analogue were necessary to measure the rates of electron transfer between the proteins and the complex. The focus of these studies was on determining how an electron is transferred through a protein when redox centers are separated by 20 to 40 Å (Durham et al. 1997). A few theoretical studies were able to detail the movement of electrons in the experimental systems (Regan et al., 1993; Beratan et al., 1991).

Another technique is the use of flavin derivatives reduced with laser light that generate reactive redox species. This technique was used extensively by Tollen et al. (1991) in the investigation of cytochrome c peroxidase.

1.3 The Use of Ru Complexes in Laser Flash Photolysis

None of the proteins in the electron transport chain are photoreactive and thus not suitable to the flash photolysis experiment unless a suitable photoinitiation reagent is present. Several schemes have been developed using ruthenium bipyridine complexes that allow laser flash photolysis to be used to investigate the electron transfer reactions. A typical reaction scheme is shown in Figure 1-3. Electron transfer is initiated, using a laser, by exciting a Ru complex attached to the protein (Durham et al., 1989). The ruthenium complex, which has a reasonably long lived excited state, injects an electron into the heme iron, converting the Fe (III) to Fe (II).. The resulting ruthenium (III) is re-reduced by a sacrificial electron donor in the

Figure 1-3: Schematic representing the reduction of the Fe^{3+} atom of a heme protein by a bound and unbound Ru^{2+} complex.
Durham, B. Millet, F. (1989) "Photoinduced Electron-Transfer kinetics
 of singly labeled ruthenium bis(bipyridine) dicarboxybipyridine
Cytochrome c Derivatives" Biochemistry 28 : 8659-8665

Ru(I) + Fe(III)

AN^+

AN

$k_{q'}$

K

AN^+

Ru(I),Fe(III)

AN

k_q

k_4

$Ru(II)^* + Fe(III)$ ⇌K⇌ $Ru(II)^*,Fe(III)$

k_1

AN AN^+

$h\nu$ k_d $\quad$ $h\nu$ k_d

Ru(III),Fe(II) →k_s→ **Ru(II),Fe(II)**

k_2

K $\quad$ K

Ru(II) + Fe(III) ⇌K⇌ Ru(II),Fe(III)

Ru(III) + Fe(II) $\quad$ Ru(II) + Fe(II)

11
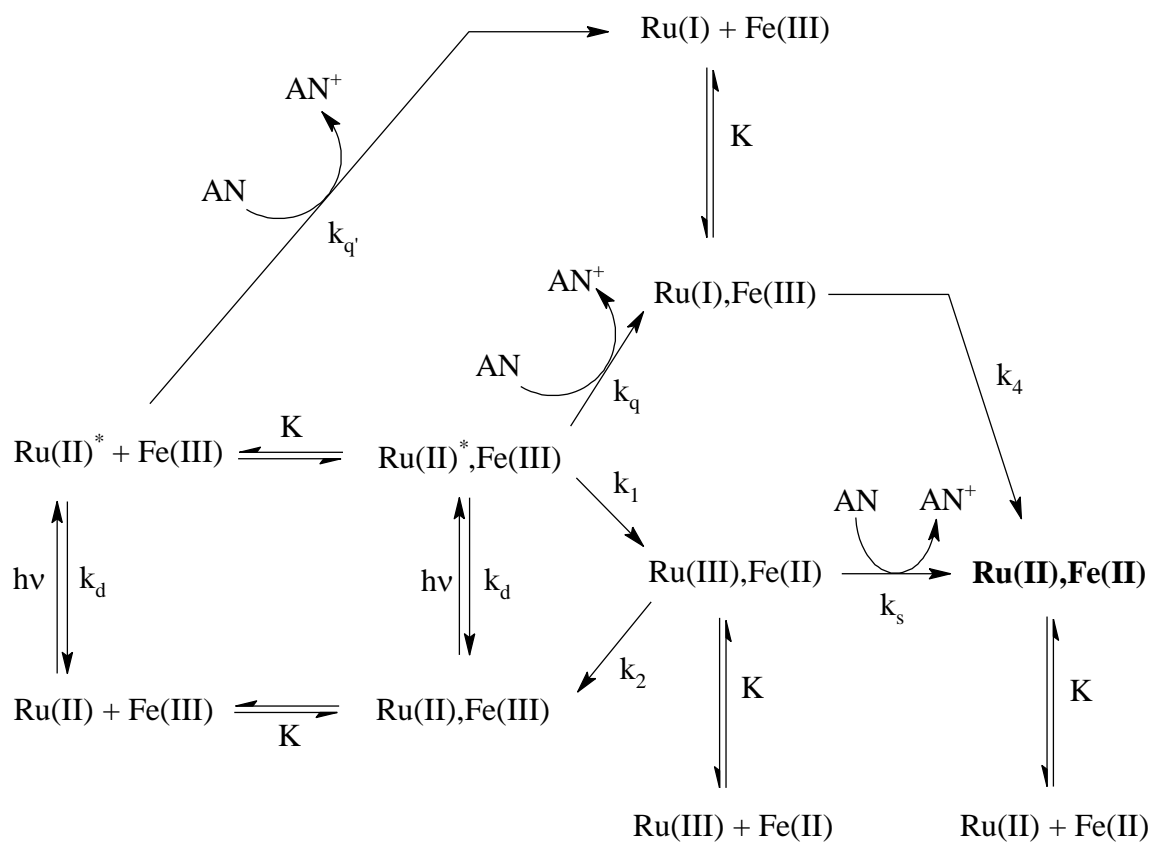
solution, and the heme is permanently reduced on the time scale of the experiment. If another

protein (e.g., a physiological partner) in the appropriate oxidation state is present in solution, the

reaction of the between the newly reduced protein and its physiological partner can be monitored

on a time scale comparable to the laser pulse, nanoseconds.

Figure 1-4: Ruthenium monomer and dimer complexes that have been used to study electron transfer reactions.

Ru monomers

Quaterpyridine complexes
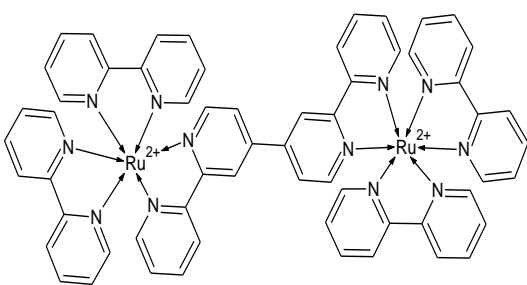
Ru₂D : Robert's dimer [Ru(bpz)₂]₂(qpy)⁴⁺

Ru(bpy)₃²⁺

Ru(bpz)₃²⁺

Ru(mobpy)₃²⁺

Ru₂Z : Sany's dimer [Ru(bpz)₂]₂(qpy)⁴⁺
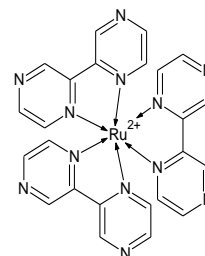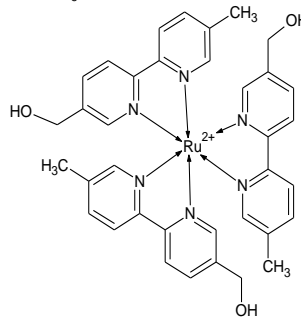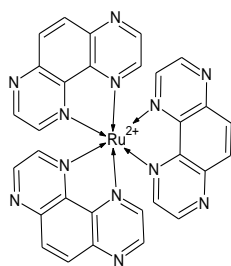
Ru(TAP)₃²⁺

Ru(HAT)₃²⁺

14
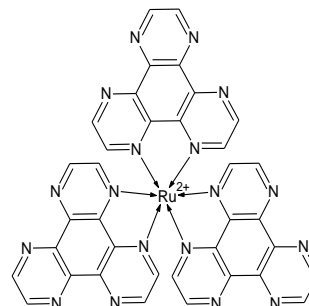
1.4 Ru Complexes used

A wide variety of Ru complexes have been used over the past few decades (Durham et al. 1989). See Figure 1-4 for examples. Some of these are covalently attached to a protein and some are simply added to the solution where they bind electrostatically to a protein and allow the laser flash photolysis experiment to proceed. In 2001, Tracey Jackson investigated whether the overall charge of the Ru complex, the type and length of the charged group, and the number of Ru nuclei can affect binding affinity. He synthesized complexes with positively charged amino groups on long, flexible aliphatic arms to see if chain length allowed the complex to better interact with the negatively charged regions of the proteins surface for tighter binding. See Figure 1-5. He showed that the binding affinity for cytochrome b_5 increases with increasing charge, but all complexes of similar charge show the same basic affinity (Jackson, 2001). See Figure 1-6.

1.5 Cytochrome b_5

The characterization of these complexes and understanding of how they interact with proteins provides insight into the reactions they facilitate and can lead to improvements in the design of new complexes. Because there is abundant data about its structure, interactions, and mechanisms, cytochrome b_5 has become a model protein for theoretical and experimental studies (Ozols 1989; Wendoloski et al., 1987; Rodgers et al., 1989; Funk et al., 1990). Cytochrome b_5 is a hemoprotein that participates in a wide variety of physiological redox reactions. They are present in animal, plant, fungi, and purple photosynthetic bacteria species. In animal tissues, the

Figure 1-5: Ruthenium complexes designed by Tracey Jackson (2001) to investigate electron transfer reactions of cytochrome b_5.
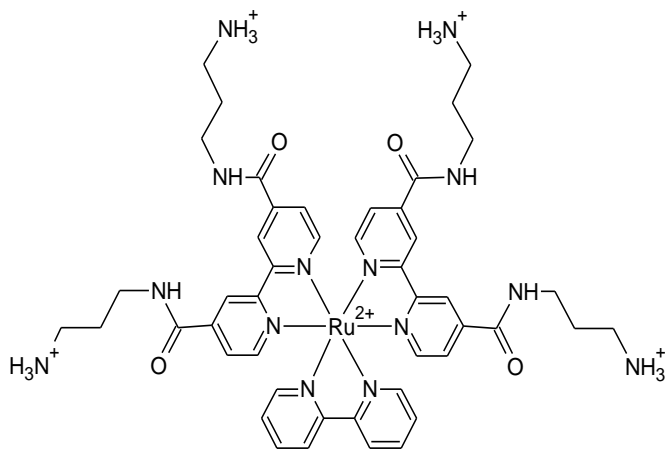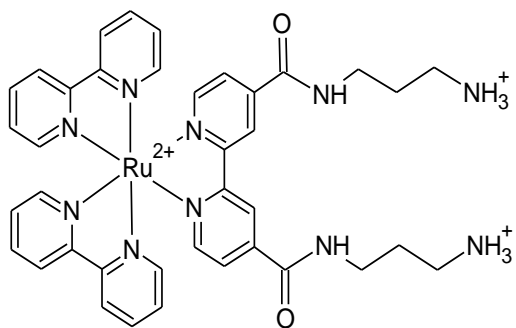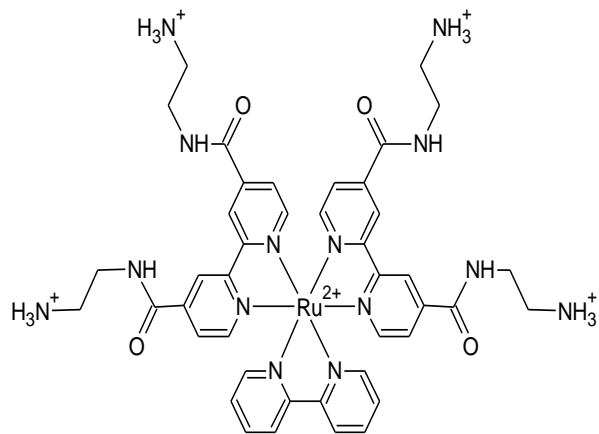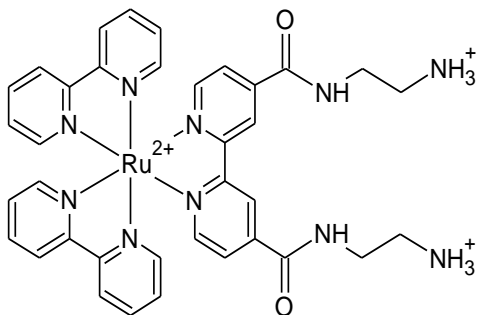
Figure 1-6: Graph of fraction bound of Tracey Jackson's ruthenium complexes vs. concentration of cytochrome b_5. Graph shows that all complexes of similar overall charge bind with the same affinity. *Jackson, Tracy (2001) "Electrostatically bound metal complexes for the study of electron transfer in metalloproteins" Dissertation, University of Arkansas, Fayetteville, AR*

sequence is highly conserved and can be found in both membrane bound and water soluble forms, each produced by alternative splicing during expression (Mathews et al., 1985).

The membrane bound form is primarily found in the endoplasmic reticulum of liver cells. It reduces unsaturated fatty acids before they enter the metabolic degradation pathways (Strittmatter et al., 1974). It also acts as an electron source for cytochrome P450 in a variety of reactions that hydroxylate toxins in order to make them more soluble and easier to degrade, which facilitates elimination (Imai et al. 1977). Cytochrome b_5 is also found on the inner surface of the outer membrane of mitochondria. It is reduced by cytoplasmic NADH-cytochrome b_5 reductase. Cytochrome b_5 then transfers an electron to cytochrome c in the mitochondria (Matlib et al., 1976).

The water soluble form is found in mammalian and avian erythrocytes. Its primary function is to reduce methemoglobin to hemoglobin using NAD^+ (Hultquist et al., 1984). If one of the hemoglobin tetramers becomes oxidized, Fe^{2+} to a Fe^{3+}, it loses its ability to bind oxygen and causes the other three to bind oxygen tighter, preventing them from releasing oxygen to tissues. This results in a condition called methemoglobinemia, which can lead to tissue hypoxia (do Nascimento et al., 2008).

The structure of rat liver microsomal cytochrome b_5 has previously been determined by x-ray crystallography (Argos, et al. 1975) and NMR (Lee et al., 1994). It has been shown that the binding affinity for ruthenium complexes increases with higher positive charges (Chaudaev et al., 2001). It was speculated that the binding location is at the negatively charged residues near the heme, which is the site for cytochrome b_5's natural substrates (Wang et al., 2003). See Figure 1-6 for an electrostatic surface potential map of cytochrome b5.

A truncated form cytochrome b_5 is commonly used where the hydrophobic tail that anchors it into a membrane is eliminated in order to increase its solubility in water. NMR studies have shown that cytochrome b_5 exists in two isoforms referred to as A (major) and B (minor) (Keller et al., 1976). The heterogeneity results from a 180˚ rotation of the heme group about the axis along the α and γ meso carbons (La Mar et al., 1981). The two isoforms differ in reduction potential by 27 mV (Sarma et al., 1996). The ratio of major to minor isoforms varies with species: chicken 20:1, calf 8.9:1, rat 6:4 (Lee et al., 1994). See Figure 1-7 for a stereo view of the heme of cytochrome b_5 and its ligating residues.

Rat liver cytochrome b_5 is unique in that it has the highest detectable heterogeneity in solution. This can give rise to 40% more resonances in ^{1}H-^{15}N HSQC spectra making resonance assignments difficult (Sarma et al., 1996). Any 2D NMR studies of rat liver cytochrome b_5 will have to take both conformers into account.

Figure 1-7: Electrostatic surface map ofcytochrome b$_5$ from PDB 1AW3 rendered with Pymol.
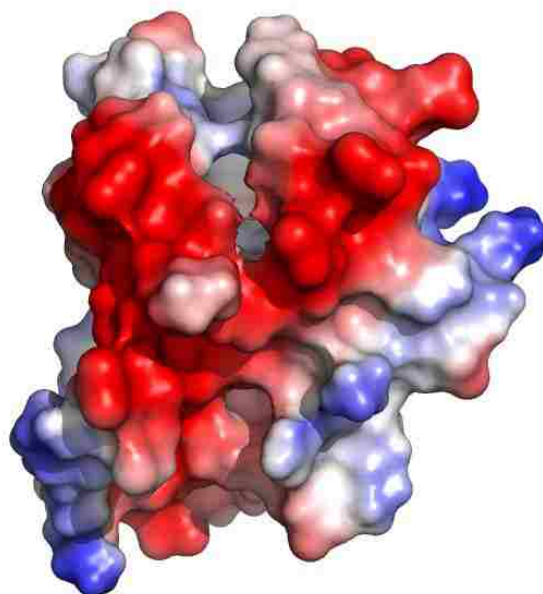
Figure 1-8: Stereoview of cyt b$_5$. Heme Fe axial ligands His 63 and His 39are shown in blue (36).

Altuve, Adriana; Silchenko, Svetlana; Lee, Kyung-Hoon; Kuczera, Krzysztof; Terzyan, Simon; Zhang, Xuejun; Benson, David R.; Rivera, Mario "Probing the Differences between Rat Liver Outer Mitochondrial Membrane Cytochrome b$_5$ and Microsomal Cytochromes b$_5$". Biochemistry 2001, 40 9469-9483
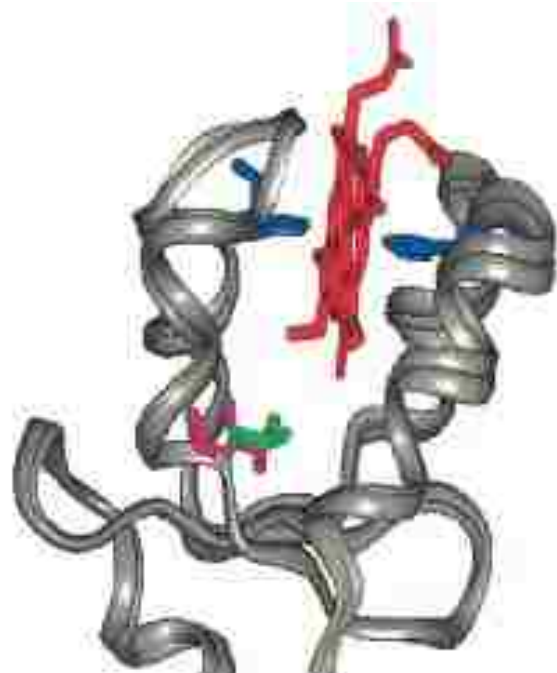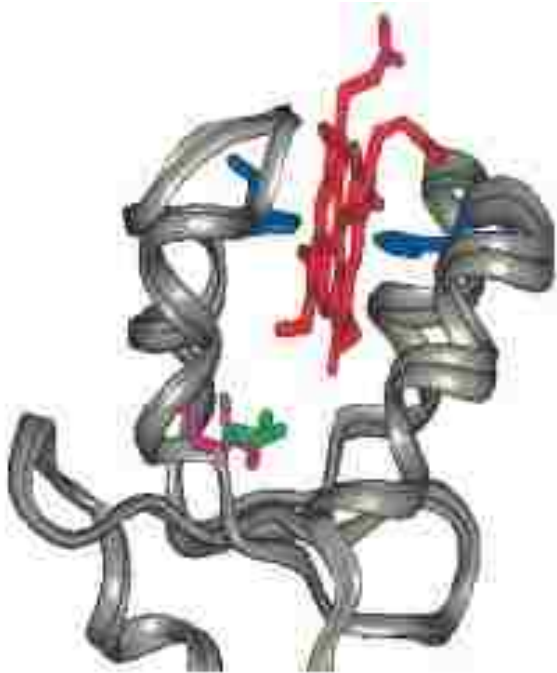
1.6 The Cytochrome b$_5$ and Cytochrome c complex

One of the most intensely studied interactions of electron transfer proteins is the complex formed between cytochrome b$_5$ and cytochrome c. Salemme (1976) was the first to propose a detailed structural model of the complex. Available crystal structures (Argos et al. 1975, Takano et al., 1973) were aligned with a least squares minimization of the distance between hemes to give a well-defined model with a stoichiometric ratio of 1:1 and four interprotein charge interactions: E44-K13, E44-K27, D60-K72, and the 6 propionate-K79 (cytochrome b$_5$ residues listed first). See Figure 1-8. This model included excluded water molecules at the binding interface and nearly coplanar hemes 8 Å apart. This model prompted the development of experimental techniques to determine the structural properties and electron transfer mechanism of the complex.

Gel permeation and ultracentrifugation studies provided the first evidence that the c-b$_5$ complex does form with a ratio of 1:1 (Stoneheurner et al., 1979). This conclusion was supported by electronic spectroscopy (Mauk et al., 1982), and NMR studies (Eley et al., 1983). Researchers used chemical modification of the lysine residues of cytochrome c along with steady state kinetics to determine which residues play a role in complex binding (Ng et al., 1977; Smith et al., 1980). Researchers also esterified the propionate groups of the heme of b$_5$ and used spectrophotometry to determine the role they play in complex formation (Reid et al., 1984, Mauk et al. 1986). Later, mutagenesis of the negatively charged residues of cytochrome b$_5$ was used in combination with hyperbaric spectroscopy to determine their involvement in the binding reaction (Rodgers et al. 1988, Rodgers et al. 1991). These studies generally supported the Salemme model of the complex, but found that different interactions might also play a role. Mauk (1986)

Figure 1-9: Proposed model of the complex formed between bovine cytochrome b_5 and horse heart cytochrome c. The model posits four electrostatic charge interactions: E44-K13, E44-K27, D60-K72, and the 6 propionate-K79 (cytochrome b_5 residues listed first).
Salemme F. (1976) "An Hypothetical Structure for an Intermolecular Electron Transfer Complex of Cytochromes c and b5" Journal of Molecular Biology 102, 563-568
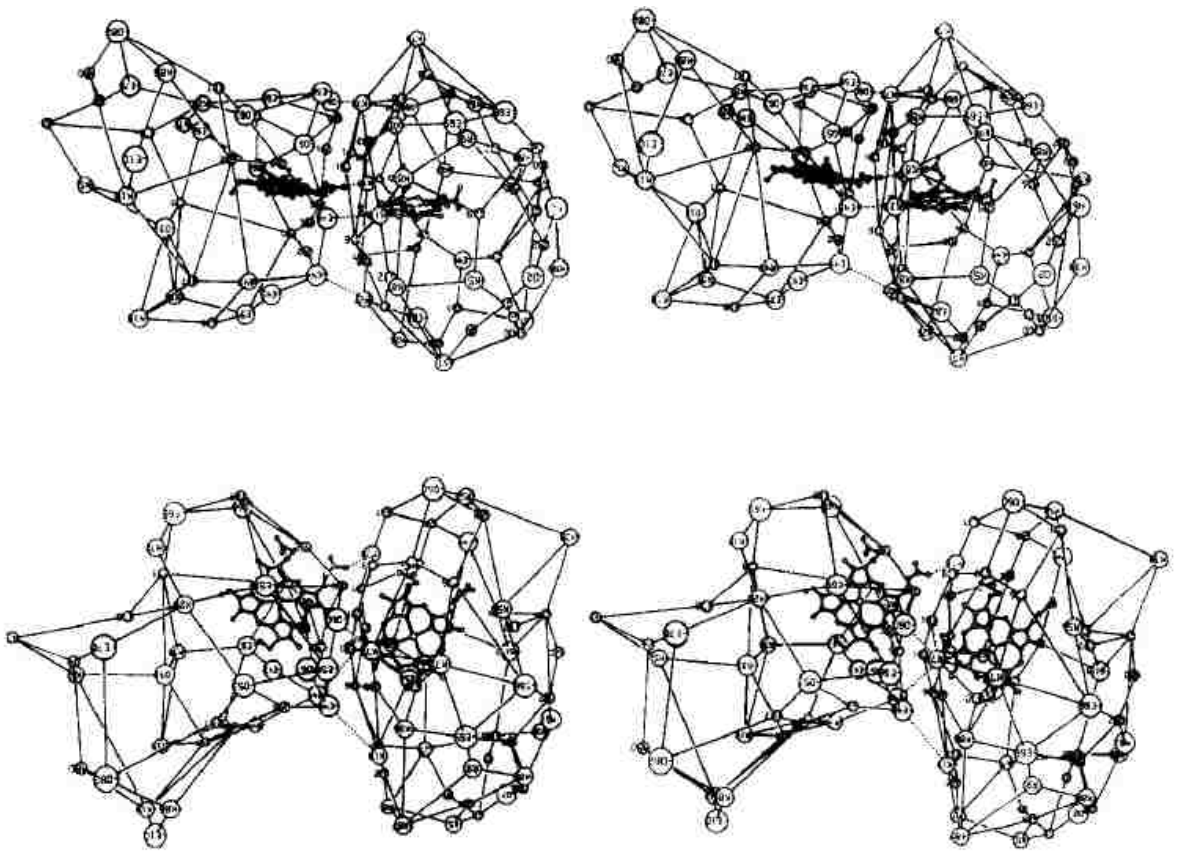
suggested that the ionic strength dependence (Stoneheurner et al., 1979) of charge transfer reaction between cytochrome c and cytochrome b_5 is likely due to five to seven interactions (Mauk et al. 1986).

It became clear that the static Salemme model did not accurately account for increasingly acquired observations of the nature of the binding between cytochrome c and cytochrome b_5 (Willie et. al., 1992). Brownian dynamic simulation studies concluded that while there is only one binding domain involved in complex formation, there are multiple docking conformations contributing to electron transfer (Northrup et al., 1993). Observations NMR titration curves and the line-broadening at higher cytochrome c concentrations suggest that a ternary complex with one cytochrome b_5 and two cytochrome c molecules may be in equilibrium with the binary complex (Whitford et al., 1990).

Volkov et al. (2005) investigated the complex formation of cytochrome b5 and cytochrome c using HSQC and modelling with the HADDOCK docking algorithm. For a description of the HSQC technique, see the following section. The researchers determined that a small patch of residues on the surface of cytochrome c is involved in the interaction. In contrast, residues all over the surface of cytochrome b_5 play a role in binding. See Figure 1-9 for a surface map of these residues. The NMR data and the docking study show a dynamic binding model with multiple conformations.

1.7 Heteronuclear Single Quantum Coherence Spectroscopy

A powerful tool in the investigation of protein binding dynamics has been the use of Heteronuclear Single Quantum Spectroscopy. The experiment was pioneered by Bodenhausen

Figure 1-10: Surface map of bovine cytochrome b_5(PDB 1CYO). Residues that show significant perturbation in the HSQC spectrum are colored red. Moderately perturbed residues are orange, andSlightly perturbed residues are yellow.
Volkov, A. (2005) "The orientations of cytochrome c in the highly dynamic complex with cytochrome b5 visualized by NMR and docking using HADDOCK" Protein Science 14:799–811
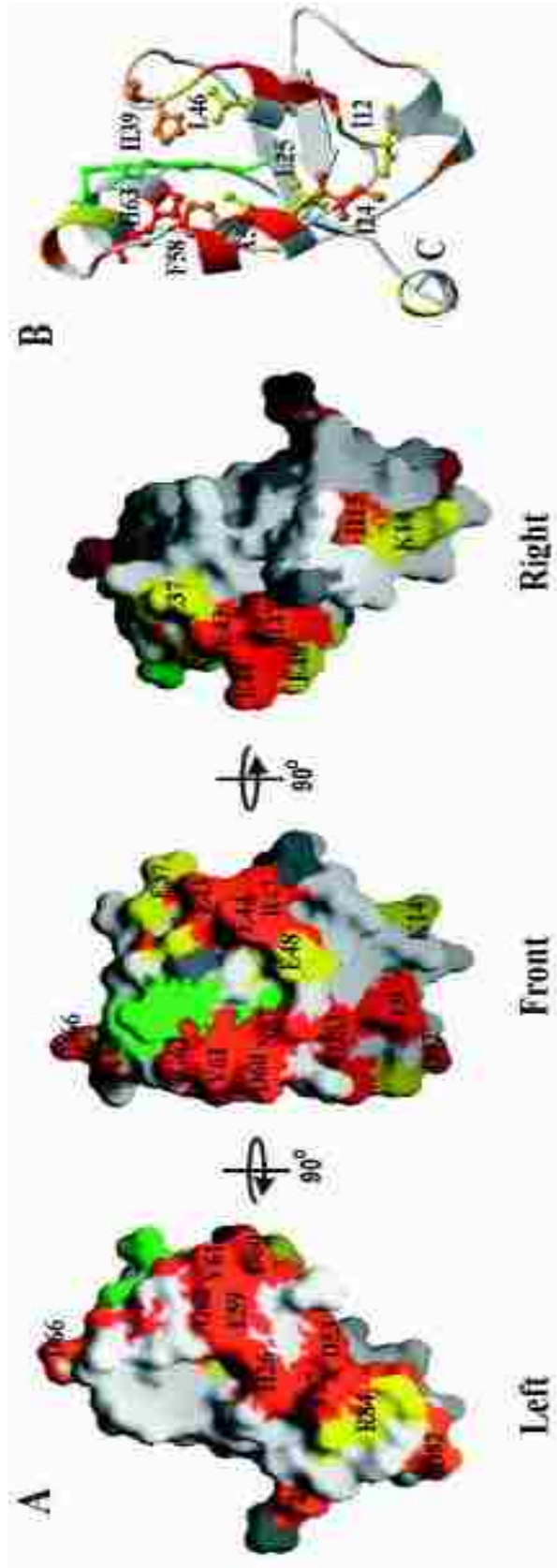
and Ruben in 1980 (Bodenhausen et al., 1980). The technique uses two dimensional NMR with proton ^{1}H as one axis and a different atom, usually ^{15}N or ^{13}C, as the other. A corresponding resonance represents a coupling from a single proton bonded to a hetero atom. In a folded protein, each backbone hydrogen is in a unique chemical environment.   So each resonance on the spectra corresponds to the backbone proton of a single residue (Cavanagh et al., 2007). For sample spectra, see Figure 3-2.

Compounds are inserted into an applied magnetic field. A radio pulse of a specific frequency causes a polarization in the nucleus of a ^{1}H atom. Next a series of radio simultaneous pulses transfers that polarization to a bonded ^{15}N nucleus. The system is allowed to relax for a certain time, before another series of pulses transfers the polarization back to the ^{1}H. As the polarization transfers back, the ^{15}N decouples from the ^{1}H, and the ^{1}H returns to its original state. The signal from the ^{1}H is recorded as it returns to equilibrium as free induction decay. The FID is processed with Fourier Transform algorithm and a two dimensional spectra is obtained (Gomathi, 1996). See Figure 1-10 for a schematic of the pulses used.

Figure 1-11: Schematic of an HSQC experiment. Black bars represent radio pulses, and the numbers above them show the angle of incidence to the magnetic moment.
http://chemwiki.ucdavis.edu/@api/deki/files/9360/=HSQC.png
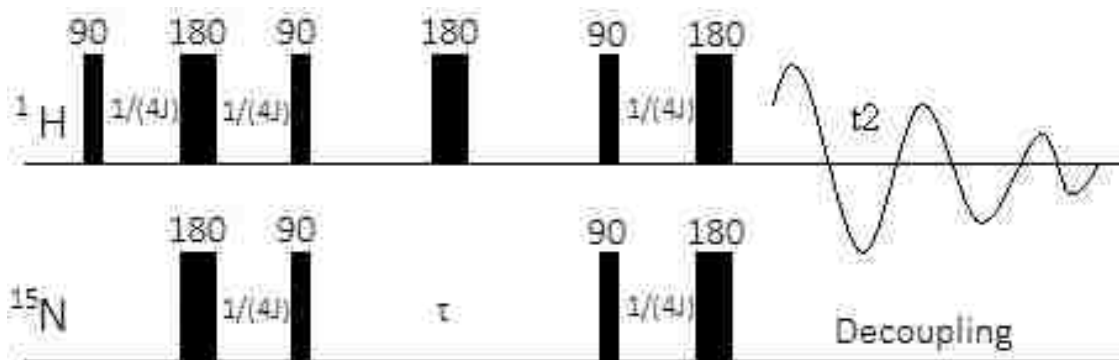
1.9 Aim of Present Work

While these compounds have been used to study electron transfer reactions for decades, little is known about how they interact with proteins. Preliminary evidence supports a simple electrostatic model. It is reasonable to assume that the complexes must bind near the heme, otherwise charge transfer would not happen (Guiles et al., 1993). The role of other forms of molecular interactions has not been investigated. Dissociation equilibrium constants have been calculated for some compounds, but the specific thermodynamic details are unknown. What is the enthalpy and entropy of binding and how can binding be improved? Do all complexes of identical charge have the same binding affinity? The present work seeks to answer these questions. The answers will help with the future design of complexes to study biological electron transfer. This work also seeks to evaluate some recently developed ruthenium dimer complexes that haven't been studied with biological systems. See Figures 1-11 and 1-12 for these new complexes.

Figure 1-12: Ruthenium dimers used in this study.
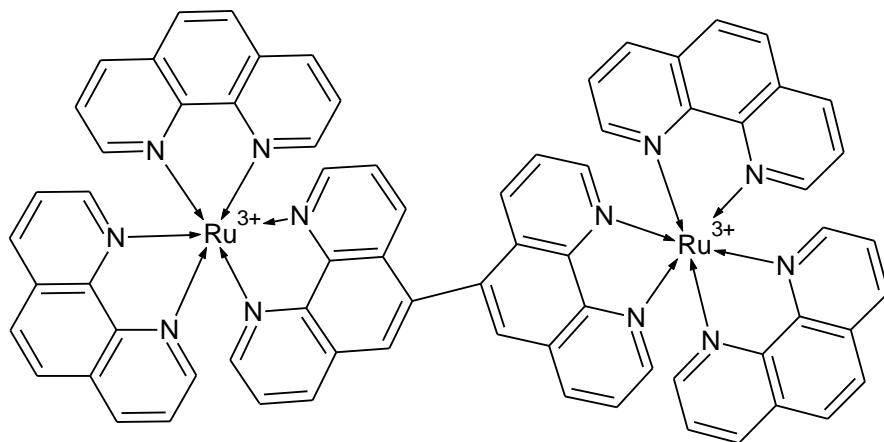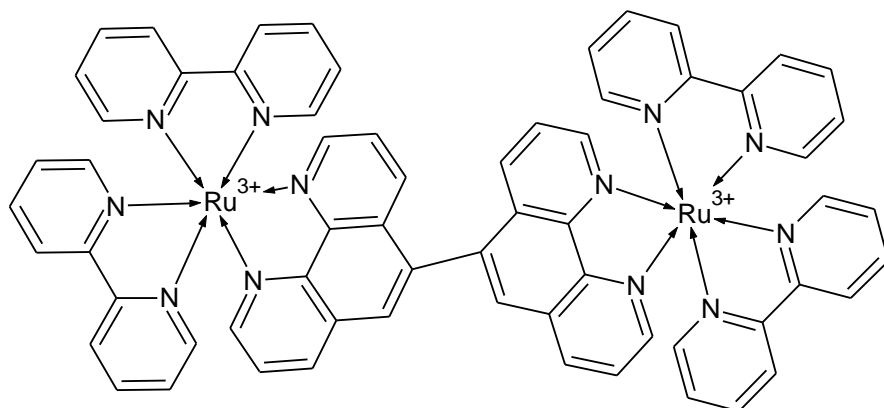
Figure 1-13: 3-D view of $[(Ru-bpy_2)_2-diphen]^{4+}$. Distance between ruthenium atoms is 11.77 Å.
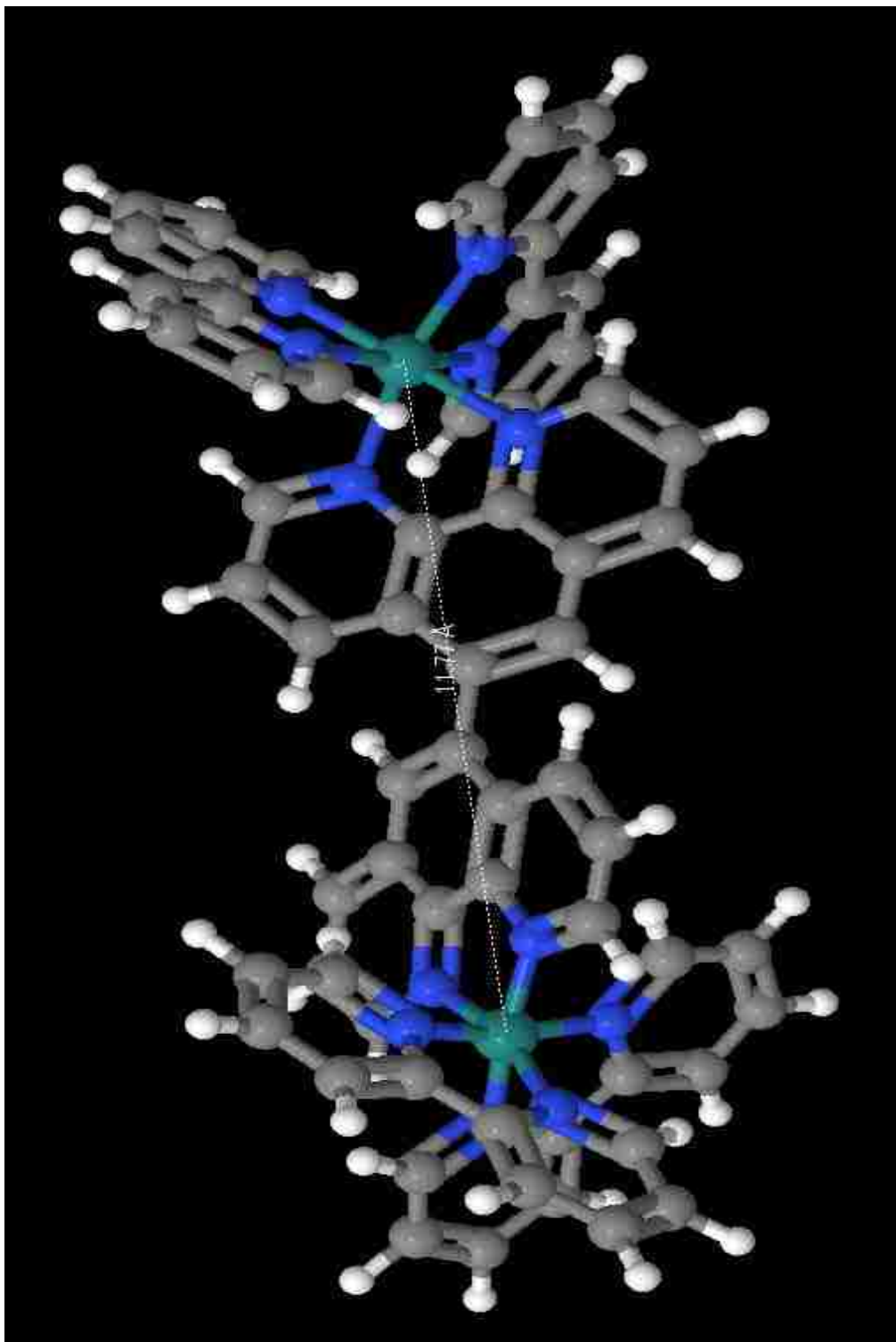
Chapter 2 - Experimental

2.1 – Preparation of Ru Complexes

Samples of $[(\text{Ru-bpy}_2)_2\text{-diphen}](\text{PF}_6)_4$ and $[(\text{Ru-diphen}_2)_2\text{-diphen}](\text{PF}_6)_4$ were obtained from other researchers in the group. For a complete description of the synthesis of these compounds, refer to the dissertations of Roland Njabon and Latisha Puckett and the master's thesis of Yinling Zhang.

Ruthenium complexes with PF_6^- counterions are not very soluble in water, so it necessary to convert the counterion in order to use them with proteins. Solid $[(\text{Ru-bpy}_2)_2\text{-diphen}](\text{PF}_6)_4$ was dissolved in a minimal amount of anhydrous acetone. $[(\text{Ru-bpy}_2)_2\text{-diphen}]\text{Cl}_4$ was precipitated by adding a few drops of saturated LiCl in anhydrous acetone. The solution was filtered and the precipitant was washed with more anhydrous acetone.

The resulting chloride salt was highly sensitive to atmospheric water and was stored in a desiccator. The salt was also photosensitive and the vial was wrapped in aluminum foil to shield it from ambient light.

2.2 - Cytochrome b$_5$ production

The plasmid for microsomal rat liver cytochrome b_5 was obtained from Dr. Steven Sligar at University of Illinois, Urbana–Champagne (Beck von Bodeman et al., 1986). 2.0 µL of the plasmid was added to 25 µL of BL21DE3 competent *E. coli* cells in a Falcon tube and incubated in an ice bath for 30 minutes. The tube was removed from the ice and heat pulsed for two

minutes at 42°C. The tube was returned to ice for two additional minutes. 0.5 ml of 2xYT broth

(4g Tryptone, 2.5 g yeast extract, 1.25 g NaCl, 250 ml DDI water) was added to the tube then

spread out over a 2xYT agar plate containing ampicillin. The plate was incubated overnight at

37 °C.

Two liters of M9 minimal media were prepared in a 6L flask with 25.6 g of

$Na_2HPO_4 \cdot 7H_2O$, 6.0 g KH_2PO_4, 1.0 g NaCl, 4ml 1M $MgSO_4$, 0.2 ml 1 M $CaCl_2$, 40 ml of 20%

glucose solution, and 2.0 g $^{15}NH_4Cl$ as the only nitrogen source (Neidhardt et al., 1974;

McIntosh et al., 1987). The media was sterilized by autoclave. Two ml of AMP100 ampicillin

solution was added to flask with the media. Two single colonies from the agar plate were

removed with sterile toothpicks and added to the flask. The flask was incubated at 37 °C

overnight on a shaker. Media remained translucent after incubation.

The next day 2 ml of 1 M IPTG (isopropyl-B-D-thiogalactoside) solution was added to

induce expression. After 10 minutes, 2ml of 17mg/ml ALA (sigma-aminolevulinic acidHCl)

was added as a precursor for heme assembly, and 2 ml of 100mg/ml $FeCl_2$ was added as an iron

source for the heme. The flask was returned to 37 °C incubation on a shaker overnight.

The next day the media appeared turbid and a gray-pink color indicating heme

expression. The media was aliquoted out into centrifuge bottles and spun at 10,000 rpm for 15

minutes. The supernatant was discarded and the weight of the cells was determined. The cells

were resuspended in 3ml of lysis buffer (50 mM Tris pH 7.5, 1mM EDTA, 100 mM NaCl) per

gram of cells. 160 μL of 10 mg/ml lysozyme solution and 32 μL of 50 mM PMSF

(phenylmethyl sulfonyl fluoride) in ethanol per gram of cells were added to the suspension. The

solution was stirred at room temperature for 20 minutes.   Four milligrams of deoxycholic acid

per gram of cells was added to the solution. The solution was stirred at 37 °C for 20 minutes

Figure 2-1: Graph of the ratio of absorbance at 412nm (heme b) to 280 nm (tryptophan indole), vs. fraction number after ion exchange gravity column. The purest fractions are from 26-29.
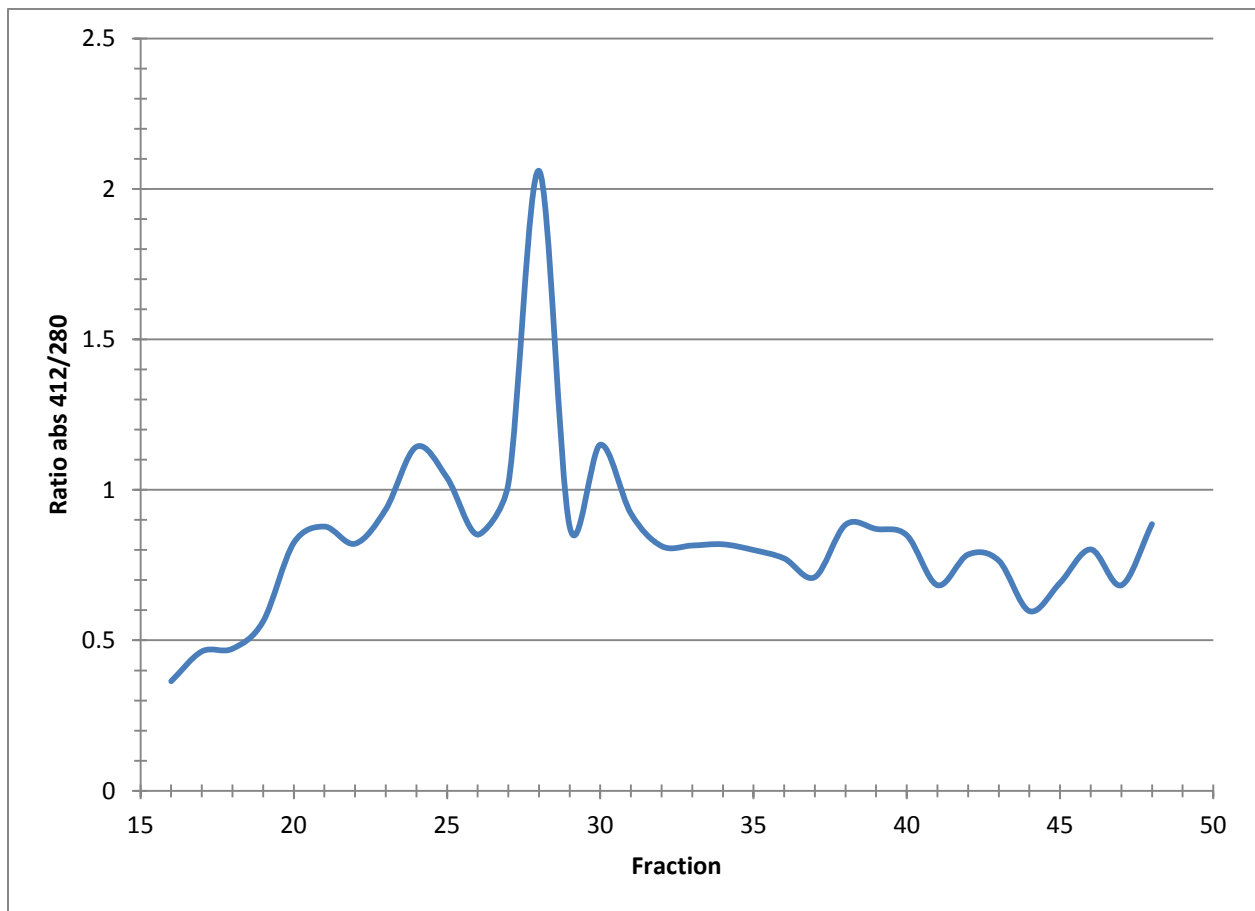
then one hour at room temperature. The solution was then frozen overnight at -80 °C. The

freeze-thaw process is important to ensure cells are disrupted properly.

The solution was thawed then centrifuged for one hour at 19,000 rpm. The pellet was

discarded and the supernatant appeared a pale red color. The solution was concentrated using

Amicon concentrators with a 5 kDa cut off at 4000 rpm down to about 30 ml. The solution was

added to an ice bath on a stir plate. Solid ammonium sulfate was slowly added while the

solution was stirred to reach a concentration of 300 g/L (about 47% saturation) then stirred for an

hour.

The solution was centrifuged at 10,000 rpm for 15 minutes and the pellet was discarded.

The solution was then added to a dialysis bag with a 6-8 kDa cut off and placed into 10L of 10

mM Tris pH 8.0 buffer. The solution was allowed to dilalyze for 24 hours at 4 °C.

A 30 cm DEAE column was equilibrated with 10 mM Tris pH 8.0 buffer and the protein

was loaded onto the column. 250 ml of 10 mM pH 8.0 Tris buffer and 250 ml of 0.3 M NaCl in

10 mM pH 8.0 Tris buffer were loaded into an auto-gradient apparatus and the gradient was

allowed to flow through the column. The protein eluted around 0.15 M - 0.2 M NaCl and

fractions were collected.

The absorbance at 412 nm and 280 nm of each fraction was measured using an HP diode

array spectrophotometer. The wavelengths represent the heme and tryptophan peaks

respectively. The ratio of absorbances was calculated for each fraction. A ratio greater than 1.0

is considered high enough purity. All fractions below this ratio were discarded. See figure 2-1.

The fractions with higher purity were pooled and the buffer exchanged into 10 mM Tris

pH 8.0 with no salt. The protein solution was loaded into a Waters 1500G HPLC with a Q12

column. A solvent bottle of 5 mM phosphate buffer pH 7.0 and a bottle of 500 mM phosphate

Figure 2-2: Absorbance spectrum of purified cytochrome b$_5$.
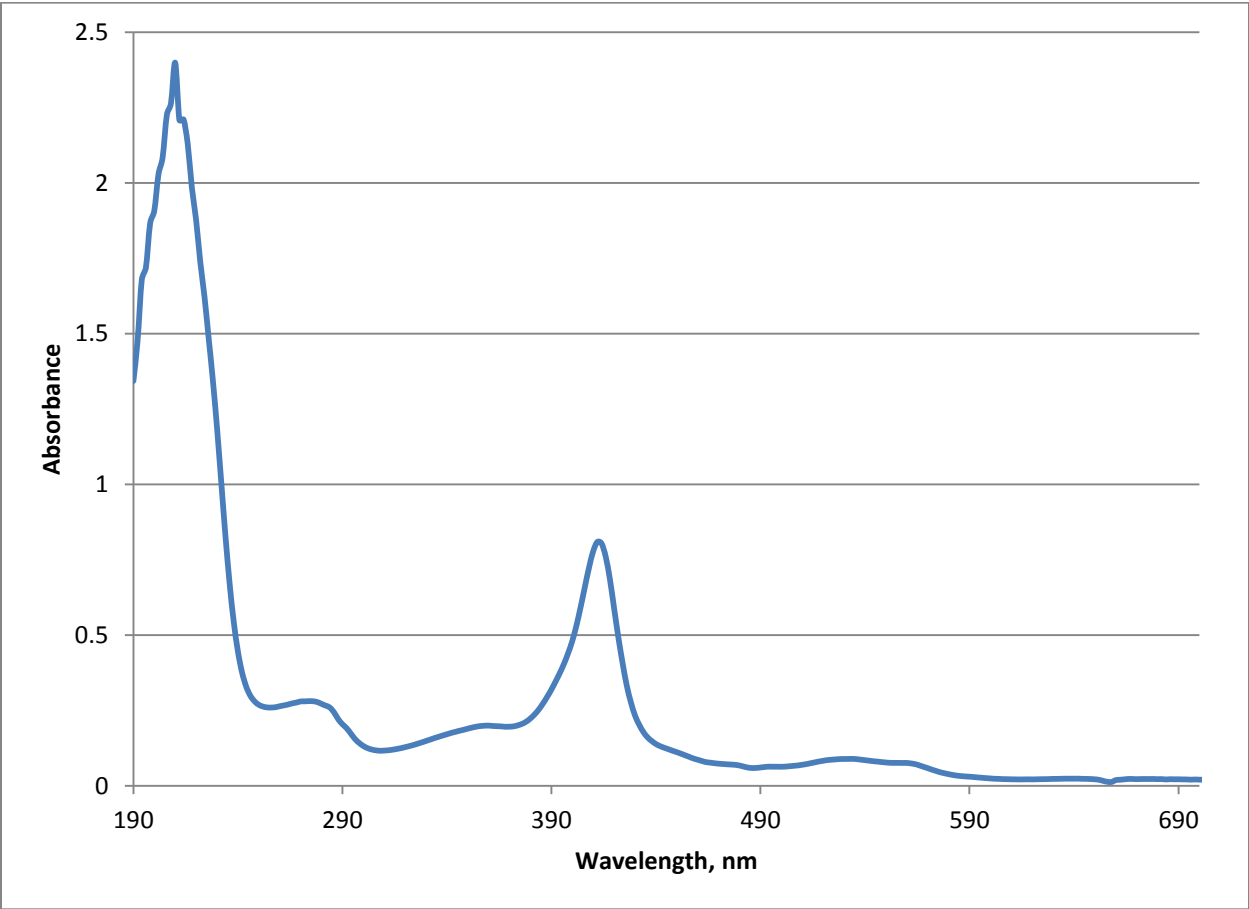
buffer pH 7.0 were programmed to run through the column as follows: minutes 0-5 ramps up to 20% 500 mM, minutes 6-45 ramps up to 60% 500 mM, minutes 46-55 ramps up to 100% 500 mM. Fractions were collected from the eluant and the ratio of absorbance at 412 nm to 280 nm were measured. Any fraction with a ratio higher than 1.0 was considered pure. The other fractions were discarded. See Figure 2-2 for a UV/Vis spectrum of the purified protein.

Fractions containing the purified protein were pooled then concentrated to a dark red color using Amicon concentrators with a 5 kDa cut off and washed with a pH 7.0 100 mM phosphate buffer.   The purity of the protein sample was verified using 20% polyacrylamide gel electrophoresis (Figure 2-3).

2.3 - NMR experiments

NMR samples were prepared by combining 51 µL of a 170 µM cytochrome b_5 solution in 10 mM phosphate buffer pH 7.0 with 9 µL of D_2O (15%) in a 5 mm diameter NMR tube. A one dimensional ^{1}H spectra was obtained on a Bruker 500 MHz NMR spectrometer and the exact chemical shift of the water peak was determined. The water peak was suppressed and a 2D HSQC spectrum was obtained with a spectral width of 8008.91 Hz for proton and 1606.60 for nitrogen atoms. Relaxation times were 0.1278 seconds for ^{1}H and 0.0651 for [15]N. The data was acquired at 40 °C using Topsin software. Further data processing was conducted with ACD/Labs ACD/NMR Processor Academic Edition version 12.01.

The HSQC spectrum of ^{15}N enriched cytochrome b_5 at 40 °C was compared to the assignments previously made by Guiles et. al., (1993) and Sarma et al., (1996). The axes from the acquired data were shifted 0.4 ppm to the left and 3.1 ppm down for the purpose of

Figure 2-3: SDS 20% polyacrylamide gel verifying purity of cytochrome b$_5$ (right channel, 11 kDa) and homemade molecular weight standards (left channel). Molecular weights of standards are, from top to bottom: 102.5 kDa, 55.8 kDa, 27.6 kDa, 6.4 kDa.
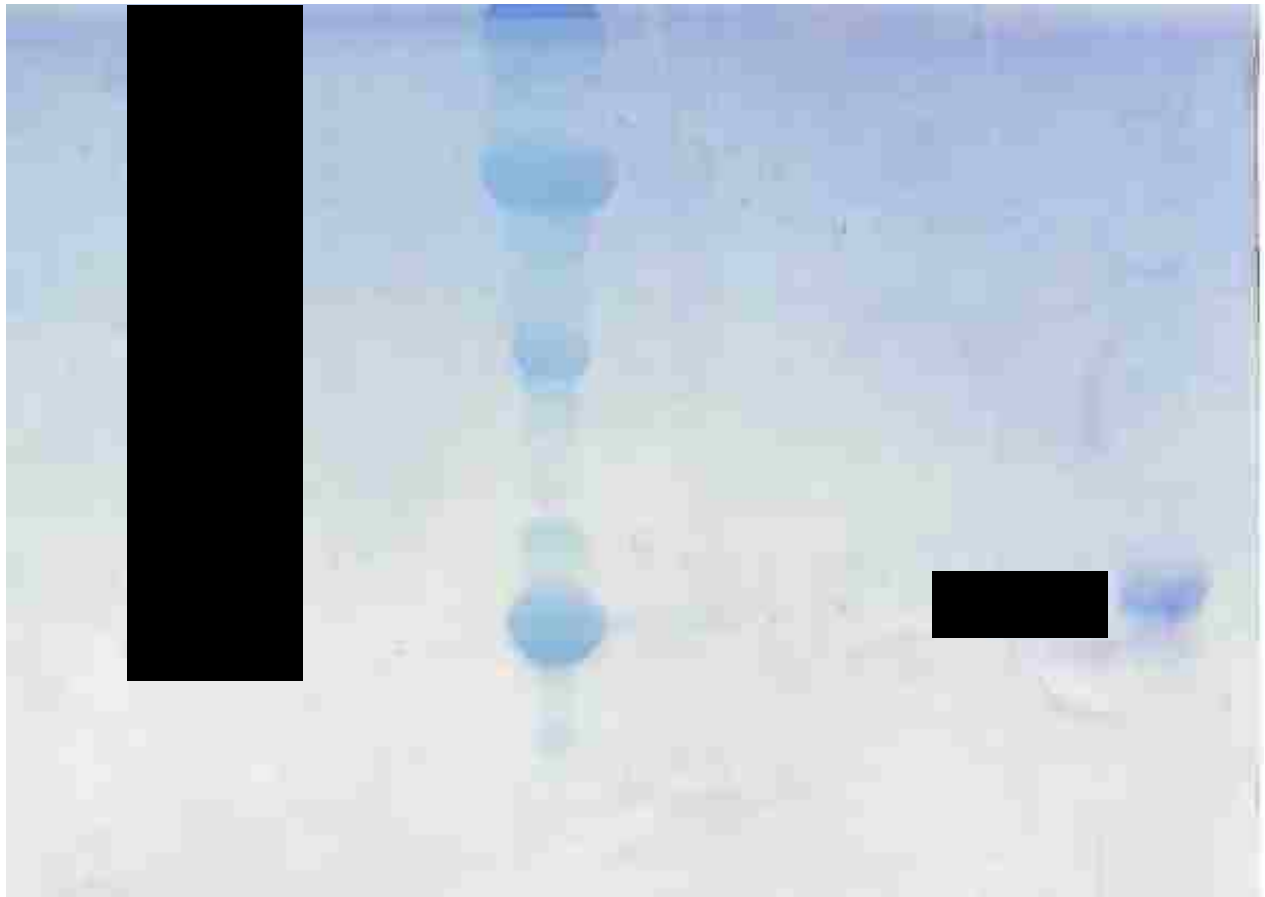
assignments only. A few assignments from that paper appear to have been mislabeled in the authors' table. See Figure 2-4. For example, residues N57 A and B, E44 A and B, and D60A appear to have assigned coordinates that do not match on the published spectra. Other errors from the coordinate table include switching of assigned residues, omission of certain residues, and coordinates given for peaks that do not appear on the published or experimental spectra. A complete list of experimentally determined peaks, the corresponding published coordinates, and observed errors from the published table can be found in Table 2-1. Spectra of the protein at both 10 mM and 100 mM phosphate buffer pH 7.0 were recorded to verify that any perturbations were not the result of ionic strength alone. See Figure 2-4 for a histogram of resonances at 10 and 100 mM buffer strength.

Adding the ruthenium bipyridine complex to the protein solution at 40 °C resulted in significant aggregation and unusable data. A series of boundary condition experiments (see section 2-3) revealed that aggregation could not be avoided at 40 °C. However, data collected at 25 °C was coherent and resulted in no observed aggregation, but the positions of the peaks at 25 °C had shifted to the point where assignments could not be made. It was necessary to reassign every peak. This was accomplished by taking spectra at 40°, 37°, 34° 31°, 28°, and 25°. Peaks were tracked at each step which allowed for accurate peak assignments at 25°.

Once accurate peak assignments were made, a 760 μM solution of ruthenium bipyridine complex $[(Ru-bpy_2)_2-diphen]^{4+}$ was titrated into 500 μL of a 10% D_2O solution of cytochrome b_5 in 10 mM phosphate buffer pH 7.0 in a 30 mm diameter NMR tube, 55 μL aliquots at a time and a NMR spectrum was acquired at each step. See Table 2-2 for exact concentrations of each species at each step.

Figure 2-4: Overlay of published spectra of cytochrome b_5 with a plot of coordinates from the published table.
Guiles, R. D.; Basus, Vladimir J.; Sarma, Siddhartha; "Novel heteronuclear methods of assignment transfer from a diamagnetic to a paramagnetic protein: application to rat cytochrome b_5" Biochemistry 1993 32, 8329-8340

12.00 11.00 10.00 9.00 8.00 7.00 6.00

110.0

G52B
A

H27

115.0

G51B
A   B G62
A

G42 A
B

V45
A

E37 A V23
B

Q(-2)Nε   G77

Q13Nε

T73B
A

S20 N57Nδ Q49 Q49N
A B

120.0

T8

V61
A

Q13 A
B S71

N57

K14
I87

E10 E38
K34 A   B
A   B

E48
T55
D53   D83
A B

L46
K16

E11
B A

Y74

Series1

125.0

H63
B A

R68B
A

Y7

D31
R47 F58

L36
R84

A50

E43
A
B

E78
E59

T33 I76

E56 AF35
V29 K18
H39   B A

L79

D17
K86 V4

A
B K72

I75

D82

D60B
A

L32
L25

I12

D3
D66

Y6
B
A I24

130.0

L9 E44
B A

H26
A

T21
B
A

B
A
W22Nε

D66

H15

K28, K89
L70

S64B
A

B
A Y30 W22
B A

K5 A88

135.0

H80

A54 A
B

L94

140.0

11.0   10.0   9.0   8.0   7.0

¹H (ppm)

¹⁵N (ppm)

Table 2-1: List of experimentally determined peaks for cytochrome b$_5$, the corresponding published coordinates, and observed errors from the published table.

Experimental			Literature		
F2 ^{1}H	F1 ^{15}N	residue	F2 ^{1}H	F1 ^{15}N	Notes:
8.308	117.743	D1	8.270	117.400	
8.073	120.123	K2	8.090	119.600	Very clustered here. Experimental and published spectra look identical.
8.189	117.634	D3	8.160	117.400	marked in a different place on the spectra in the paper. Confidence low
7.629	120.595	V4	7.590	120.700	
8.047	126.753	K5	8.000	126.500	
8.103	121.587	Y6	8.060	121.400	
8.672	118.281	Y7	8.620	118.000	
9.115	115.032	T8	9.130	114.800	
9.758	123.798	L9	9.700	123.400	
8.389	117.002	E10	8.350	116.800	
7.648	118.325	E11	7.610	118.200	
8.440	121.477	I12	8.370	121.200	
8.113	115.098	Q13	8.070	114.900	
7.299	115.448	K14	7.230	115.100	marked in a different place on the spectra in the paper. Switched with I87. Confidence low
7.643	121.383	H15	7.600	121.100	
7.455	117.156	K16	7.420	116.800	
8.083	121.083	D17	8.060	121.000	
		S18	7.390	113.200	no sign of this peak on the experimental or literature spectrum. Not sure what they are defining. Possible multiple in K14, I87 cluster

Experimental			Literature		
F2 ^{1}H	F1 ^{15}N	**residue**	F2 ^{1}H	F1 ^{15}N	Notes:
8.072	119.398	K19	8.040	119.200	Very clustered here. Experimental and published spectra look identical.
7.528	113.171	S20	7.480	112.800	
8.711	122.922	T21	8.660	122.400	marked in a slightly different place on the spectra in the paper. Confidence high
8.619	126.797	W22A	8.580	126.600	A and B peaks on top of one another
		W22B	8.590	126.600	
8.412	112.931	V23A	8.390	112.400	marked opposite B and A from paper to spectrum labels
8.456	112.199	V23B	8.420	111.800	marked opposite B and A from paper to spectrum labels
7.936	122.506	I24A	7.870	122.200	
7.871	122.047	I24B	7.820	121.700	
8.579	122.453	L25A	8.550	122.300	
8.610	122.540	L25B	8.580	122.400	
9.252	125.615	H26A	9.210	125.400	
9.291	125.615	H26B	9.230	125.400	
8.550	107.658	H27	8.500	107.500	
8.318	121.674	K28A	8.260	121.800	
		K28B	8.280	122.800	no sign of this peak on the experimental or literature spectrum. Not sure what they are defining.
8.320	120.886	V29A	8.270	120.600	
8.365	121.018	V29B	8.320	120.800	
8.792	126.162	Y30A	8.740	125.800	
8.836	126.315	Y30B	8.790	126.000	

Experimental		Literature			
F2 ^{1}H	F1 ^{15}N	residue	F2 ^{1}H	F1 ^{15}N	Notes:
8.137	119.270	D31	8.050	118.200	marked in a different place on the spectra in the paper. Likely in the K19, K2, F35 cluster. Confidence low
8.499	121.871	L32A	8.490	121.600	
		L32B	8.450	121.900	Very clustered here. They saw four peaks where I only saw two. Experimental and published spectra look identical.
8.761	119.617	T33	8.710	119.500	
9.269	117.253	K34A	9.140	116.900	
9.146	117.296	K34B	9.250	116.900	
8.128	119.792	F35A	8.110	119.500	Very clustered here. Experimental and published spectra look identical.
8.072	119.398	F35B	8.040	119.200	Very clustered here. Experimental and published spectra look identical.
7.830	119.048	L36A	7.770	118.700	
7.696	118.522	L36B	7.620	118.400	
8.576	112.440	E37	8.530	112.200	
8.308	117.743	E38A	8.270	117.400	
8.269	117.743	E38B	8.230	117.400	
8.847	120.033	H39A	8.790	119.900	
8.708	119.704	H39B	8.650	119.500	
		P40			
		G41			not defined anywhere
10.272	111.958	G42A	10.230	111.700	
10.503	112.265	G42B	10.480	112.000	

Experimental			Literature		
F2 ^{1}H	F1 ^{15}N	**residue**	F2 ^{1}H	F1 ^{15}N	Notes:
9.906	120.799	E43A	9.920	120.600	
9.970	121.018	E43B	9.970		No 15N coordinate published in table
9.557	123.885	E44A	9.570	121.800	marked in a different place on the spectra in the paper. Confidence low
9.596	124.039	E44B	9.610	121.900	marked in a different place on the spectra in the paper. Confidence low
9.318	113.237	V45A	9.270	112.900	
9.243	112.177	V45B	9.180	111.800	
7.377	116.674	L46A	7.320	116.300	
7.372	116.937	L46B			Spectra has two forms labled but only one published in table
8.348	118.128	R47A	8.320	117.800	
8.212	118.172	R47B	8.180	117.800	
8.172	116.783	E48A	8.130	116.600	
8.058	116.543	E48B	8.010	116.400	
6.757	113.200	Q49A	6.690	112.800	
6.726	113.030	Q49B	6.670	113.000	
6.923	120.865	A50A	6.870	120.600	
6.845	120.427	A50B	6.800	120.200	
9.352	109.353	G51A	9.320	109.100	
9.321	108.762	G51B	9.280	108.500	
7.403	104.637	G52A	7.360	104.400	
7.267	104.265	G52B	7.220	103.800	
8.342	117.524	D53A	8.300	117.400	

Experimental			Literature		
F2 ^{1}H	F1 ^{15}N	residue	F2 ^{1}H	F1 ^{15}N	Notes:
8.382	117.239	D53B	8.350	117.300	
8.426	129.271	A54A	8.420	129.000	
8.516	130.124	A54B	8.530	129.900	
7.952	117.406	T55A	7.920	117.200	
7.891	117.277	T55B	7.840	117.000	
8.610	119.310	E56	8.580	117.300	marked in a different place on the spectra in the paper. Confidence low
7.756	116.411	N57A	7.660	114.200	marked in a different place on the spectra in the paper. Confidence medium
7.659	116.608	N57B	7.590	114.400	marked in a different place on the spectra in the paper. Confidence medium
8.159	118.413	F58A	8.130	116.300	marked in a different place on the spectra in the paper. Confidence low
8.078	118.128	F58B	8.000	116.100	marked in a different place on the spectra in the paper. Confidence low
8.945	119.507	E59	8.890	119.400	
9.132	122.266	D60A	9.050	121.800	marked in a different place on the spectra in the paper. Probable typo. Confidence high
9.043	121.959	D60B	8.970	122.100	
8.211	114.594	V61A	8.100	114.300	marked opposite B and A from paper to spectrum lables
8.033	115.120	V61B	7.930	114.800	marked opposite B and A from paper to spectrum lables
8.929	109.040	G62A	8.850	108.600	
8.918	108.777	G62B			Spectra has two forms labled but only one published in table
10.636	118.785	H63A	10.690	118.600	

Experimental			Literature		
F2 ^{1}H	F1 ^{15}N	residue	F2 ^{1}H	F1 ^{15}N	Notes:
10.703	118.872	H63B	10.740	118.700	
11.696	126.469	S64A	11.630	126.000	looks fine. confidence high
11.498	126.075	S64B	11.430	125.600	looks fine. confidence high
8.847	120.033	T65	8.810	119.700	
8.312	122.309	D66A	8.270	122.100	
8.226	121.674	D66B	8.170	121.500	
8.853	124.323	A67A	8.830	124.000	marked opposite B and A from paper to spectrum lables
8.900	124.323	A67B	8.790	124.000	marked opposite B and A from paper to spectrum lables
9.202	118.741	R68A	9.160	120.600	marked in a different place on the spectra in the paper. Probable typo. Confidence high
9.079	118.457	R68B	9.000	118.200	
8.981	123.404	E69A	8.950	123.200	
9.062	123.163	E69B	9.030	123.000	
8.429	122.069	L70A	8.360	121.800	
8.521	122.069	L70B	8.470	121.800	
8.348	113.325	S71A	8.310	113.200	
8.434	113.544	S71B	8.410	113.400	
7.272	120.420	K72A	7.230	120.100	
7.436	120.996	K72B	7.390	120.700	
7.717	112.308	T73A	7.670	112.000	
7.713	112.071	T73B	7.670	111.700	
7.433	117.659	Y74A	7.390	117.500	

Experimental			Literature		
F2 ^{1}H	F1 ^{15}N	**residue**	F2 ^{1}H	F1 ^{15}N	Notes:
7.582	117.803	Y74B	7.550	117.500	
6.803	120.558	I75A	6.760	120.400	
6.847	120.777	I75B	6.800	120.600	
8.610	119.310	I76A	8.590	119.000	
8.741	119.245	I76B	8.640	119.100	
7.365	110.428	G77	7.280	110.100	
9.040	118.916	E78	8.890	118.600	
8.733	123.338	L79	8.680	123.200	
9.054	130.715	H80	9.010	130.400	
		P81			
11.007	121.018	D82	10.980	120.800	
8.197	115.660	D83	8.160	115.300	marked in a different place on the spectra in the paper. Confidence low
7.375	119.748	R84	7.340	119.500	
7.799	125.527	S85	7.780	125.400	not apparent on published spectra
7.623	121.149	K86	7.600	120.800	
7.282	114.741	I87	7.260	114.600	marked in a different place on the spectra in the paper. Switched with K14. Confidence low
7.779	126.600	A88	7.820	126.100	
8.499	121.871	K89	8.470	121.600	
		P90			
		S91			not defined anywhere

Experimental			Literature		
F2 ^{1}H	F1 ^{15}N	residue	F2 ^{1}H	F1 ^{15}N	Notes:
		E92	7.780	126.400	no sign of this peak on the experimental or literature spectrum. Not sure what they are defining.
8.211	114.594	T93	8.110	114.300	
7.902	130.803	L94	7.840	130.400	

The perturbations were calculated using the quadratic formula with the difference in coordinates. A correction factor of 0.2 was applied to N-axis perturbations in order normalize it with the ^{1}H coordinates.

2.4 – Aggregation Assay

To determine the boundary conditions for aggregation, an Omega MPS10 Series Melting Point Apparatus was used. Ruthenium bypyridine complex solutions of concentrations from 100 μM to 1000 μM in 10 mM phosphate buffer pH 7.0 were combined with a 170 μM solution of cytochrome b_5 in 10 mM phosphate buffer pH 7.0. A few microliters of the mixture were added to a capillary tube with one end sealed. The capillary tube was inserted into the melting point apparatus, and the solution was observed under magnification for aggregation as the temperature was slowly raised from 25 °C to 40 °C. Some mixtures were also preheated in a 40 °C water bath, centrifuged, and the supernatant was observed in the melting point apparatus. The exact temperature at each concentration when aggregation occurred was recorded.

2.5 - UV/visible Spectroscopy

All UV/visible spectroscopy data was acquired on an HP model 8452A diode array spectrophotometer. A deuterium lamp served as the light source and was allowed to warm up at least 30 minutes prior to ensure maximum intensity. A one centimeter quartz cuvette was used in all measurements. Protein concentrations were determined using absorbance measurement at

Table 2-2: Exact concentrations of cytochrome b_5 and (Ru-bpy$_2$)$_2$-diphen at each step of titration during NMR acquisition.

Concentration of b_5 μM	Concentration of Ru complex μM	Total volume of solution μL	Ratio of Ru complex to b_5
153.0	0	500	0
137.8	75.3	555	0.546
125.4	137.0	610	1.09
115.0	188.6	665	1.64
106.3	232.2	720	2.18

412 nm with an extinction coefficient of 117,000 M^{-1} (Wang et al., 2003). Ruthenium dimer concentrations were measured at 453 nm with an extinction coefficient of 28,500 M^{-1} (Puckett, 2015). Solutions were diluted from 10:1 to 100:1 so that no absorbance measurement was above 1.0 absorbance units in order to ensure accuracy.

2.6 – Isothermal Calorimetry

Calorimetry studies were conducted using a Microcal VP-ITC calorimeter. The protein concentration was 60.21 μM and ruthenium bipyridine complex concentration was 955 μM for a ratio of 15.86:1 ligand to protein. The complex solution was injected into the cell in increments of 40μL increments. The heat of dilution was determined by injecting the Ru complex into water. The heat of dilution was subtracted from the heats determined in the complex to protein experiment. The accuracy of the instrument was checked by running a water to water experiment. The heats determined from the complex to protein experiment were best fit using a single binding site model. The coefficient of determination,r^2, was determined to verify the validity of the model. From this fit the Origin 75K2 software Version 7.0383 was used to calculate the values for the stoichiometric binding ratios, the heat of binding, and the entropy of binding.

2.7 - Laser experiments

All samples were excited with the third harmonic (355 nm) from a Nd:YAG laser (QuantaRay model DCR-1) with a 10 ns pulse width. A 2.5 cm plano convex lens 100 cm focal

length was used to focus the beam into the sample. A PMT perpendicular to the beam was used

to monitor emission lifetimes at 600 nm. A high pass filter was placed in front of the PMT to

minimize scatter light from the laser. The signal was recorded on a Lecroy 5462 digital

oscilloscope. More than 100 transients were averaged to improve the signal to noise ratio. The

data from the oscilloscope was transferred to a PC and processed using software developed in-

house (Jackson, 2001).   The data was fit to a two exponential model.

Microsoft Visual Basic 6.0 was used to fit the data with successive integration

algorithms. SI fitting has the advantage of making the parameters of an exponential expression

linear, eliminating errors from the fitting process (Matheson, 1987). For a complete discussion

of the SI fitting process and examples of code employed, see the appendix of Tracey Jackson's

dissertation (Jackson, 2001).

For biphasic emission decay, the emission can be expressed as:

$$E_t = E_0 \cdot (A_1 \cdot e^{-k_1 t} + A_2 \cdot e^{-k_2 t}) \hspace{2cm} \textbf{Equation 2-1}$$

where E_t is the emission at time t, E_0 is the emission immediately after excitation by the laser, k_1

and k_2 are the rate of decay of each phase, and A_1 and A_2 are the amplitude of each phase of

emission (Havens, 2010).   The ratio of the amplitudes of each phase corresponds to the ratio of

bound to unbound species. See section 3-3 for a description of how those ratios are used to

determine equilibrium dissociation constants.

Samples were prepared in 1 mM phosphate buffer solution at pH 7.0 in a 1 cm glass

cuvette. Protein concentrations ranged from 20 µM to 40 µM. Ru dimer concentrations were

about 5-6 µM. Measurements were taken at 9°, 21°, and 29° C.

2.8 – Modeling

The structure for cytochrome b_5 was obtained from the 1AW3 file from the RCSB Protein Data Bank (Arnesano et al., 1998). RasMol software version 2.7.2.1.1 was used for all rendering.

All ruthenium complexes were drawn with ACD Labs ChemSketch software version 12.0 and used a simple 3-D optimization. The molecules were then rendered in RasMol 2.7.2.1.1. All distance calculations for both the protein and small molecule were done with RasMol.

Chapter 3 – Results

3.1 NMR Analysis

The HSQC spectrrum of ^{15}N enriched cytochrome b_5 was obtained in both 10 mM and 100 mM phosphate buffer to ensure that ionic strength did not produce any significant changes to the peak coordinates. The two spectra were essentially identical. Figure 3-1 shows the histogram of the difference in peak coordinates for each residue. All differences were minimal.

The HSQC spectra for cytochrome b_5 at 25 °C and 40 °C were compared. Figure 3-2 shows the histogram of the difference in peak coordinates for each residue. Several resonances show a significant movement of the protein backbone over the temperature range. This is the expected result as the tertiary structure of the protein would be perturbed at higher temperatures. Figure 3-3 shows a scatter plot of the coordinates of each peak at the two temperatures. While some of the peripheral resonances show significant movement, their assignments are still obvious. However, the assignments for resonances in the clustered center area are not as obvious, which is why it was necessary to obtain spectra over a gradual temperature change. Figure 3-4 shows the spectra at each temperature over the range.

As the ruthenium bipyridine dimer was titrated into the cytochrome b_5 solution, some resonances gradually moved. These resonances correspond to the residues whose backbone N-H resonances are shifted in the presence of the complex. Figure 3-5 shows the movement of glycine 42 of both isoforms as more Ru is added. It is interesting to note that peaks did not move after the second addition. This implies that at concentrations higher than 137.0 µM, the binding sites of the protein are effectively saturated and no more binding is taking place.

Figure 3-1: Histogram of perturbations of the HSQC spectrum of cytochrome b$_5$ in 10 mM and 100 mM phosphate buffer.

Histogram of cyt b5 at 100mM vs. 10mM buffer
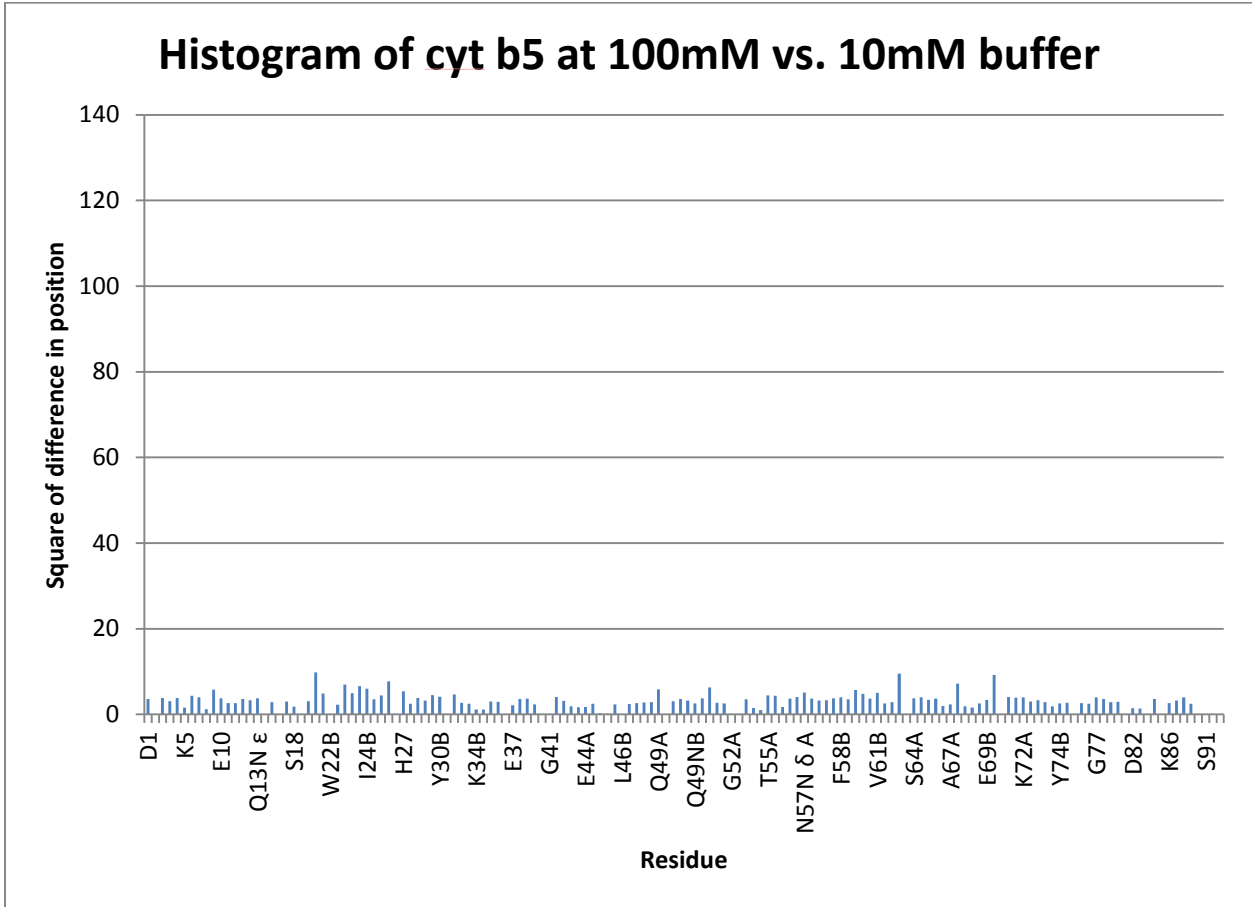
Figure 3-2: Histogram of perturbations of the HSQC spectrum of cytochrome b_5 in 25 °C and 40 °C.

Histogram of cyt b5- 25°C vs 40°C
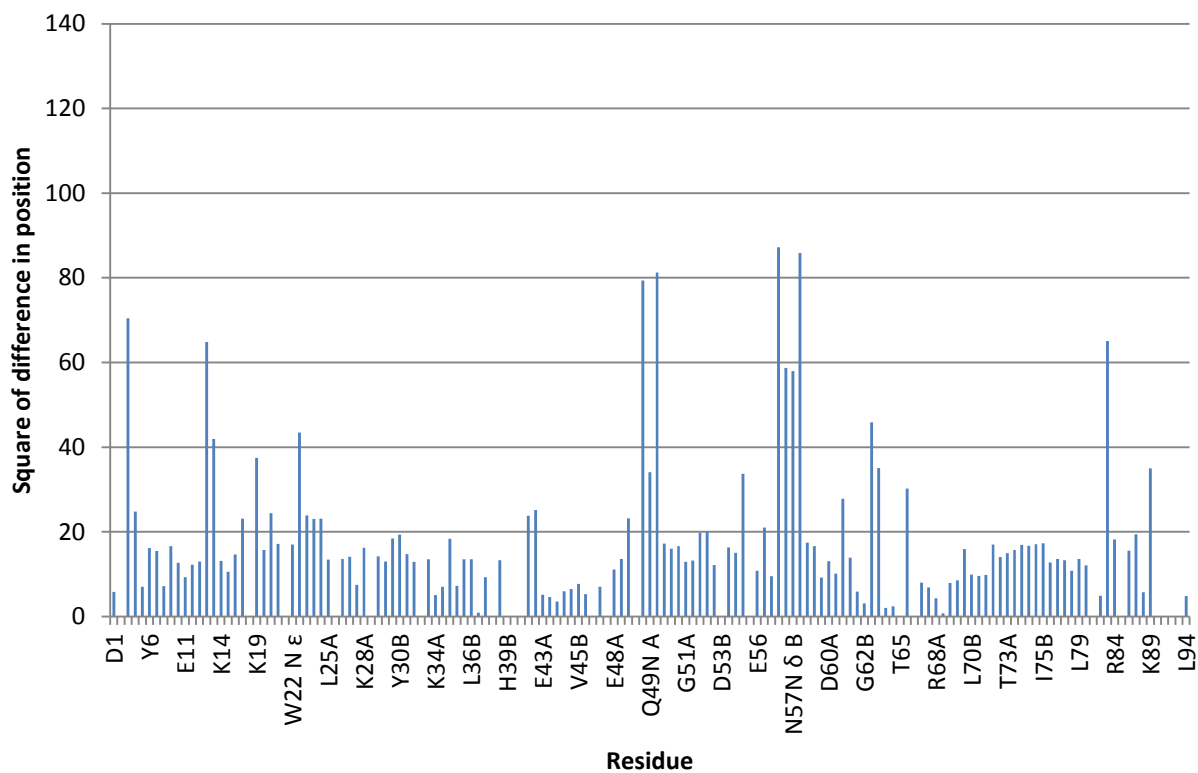
Figure 3-3: Scatter plot of the coordinates of the HSQC spectrum of cytochrome b5 in at 25 °C and 40 °C.

Scatter plot of the coordinates of cyt b5- 25°C vs 40°C
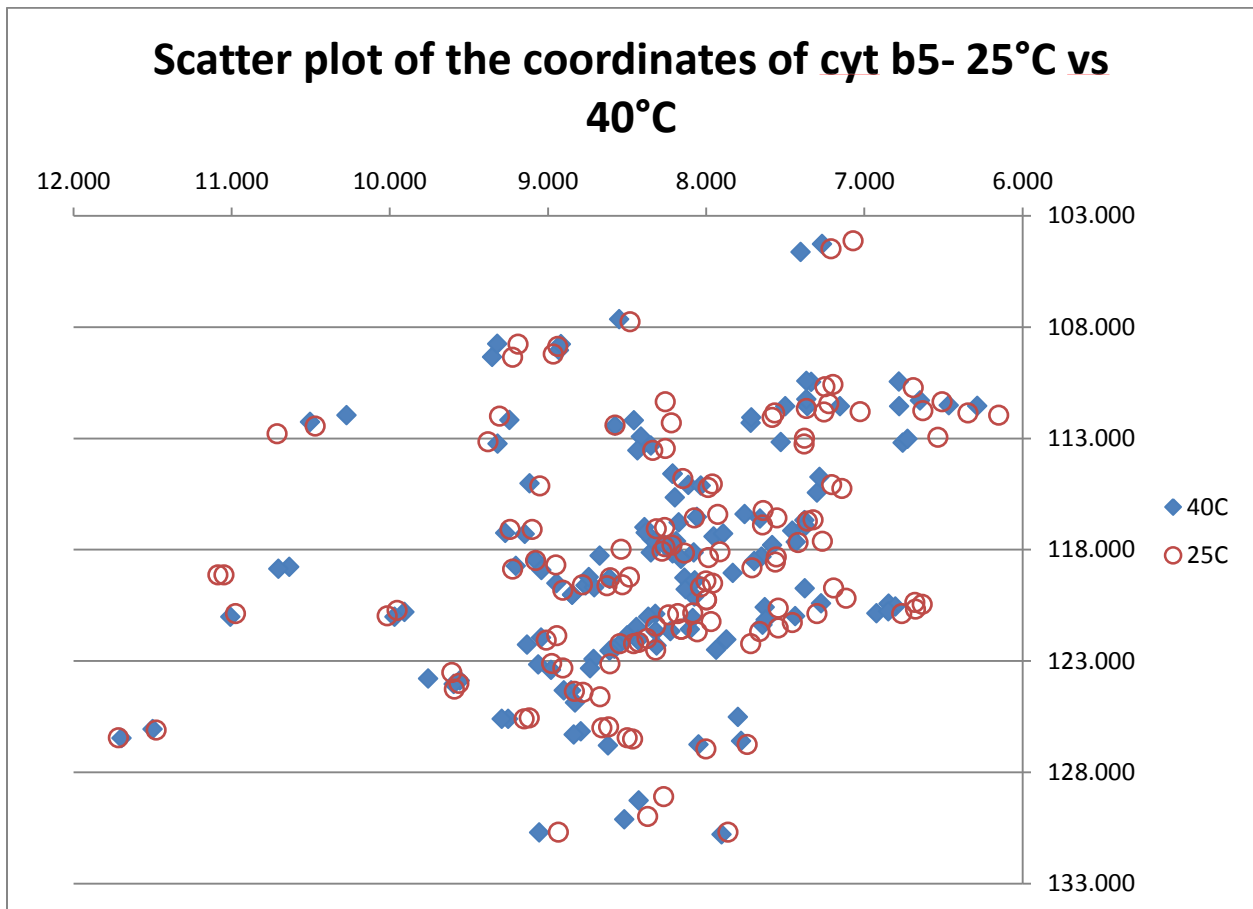
Figure 3-4: HSQC spectra of cytochrome b$_5$ at temperatures from 40°-25°.
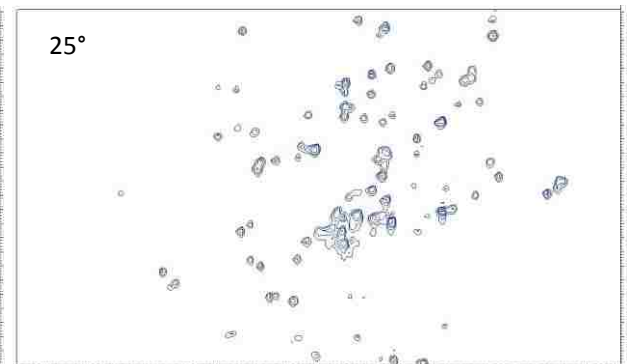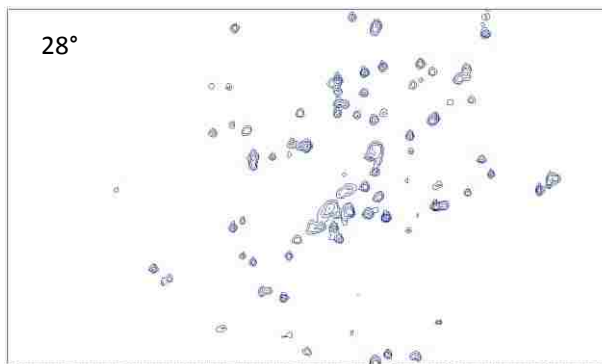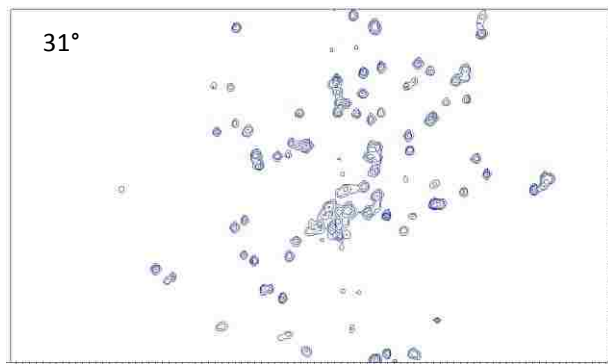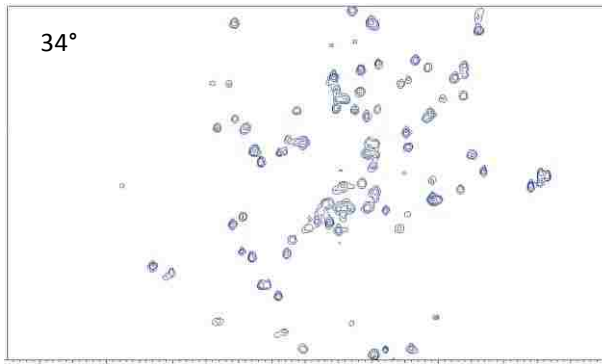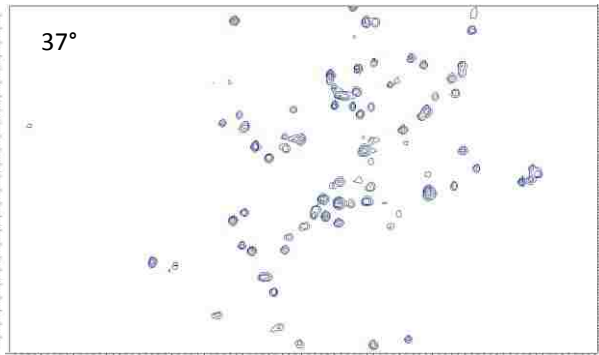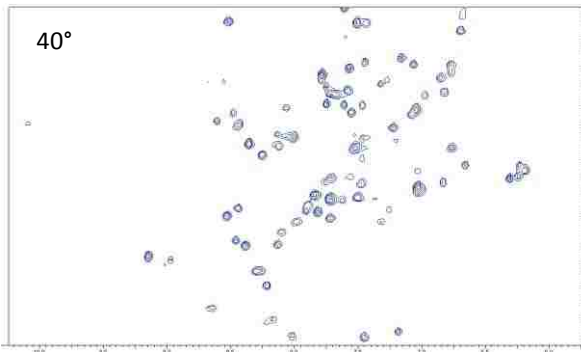
Figure 3-5: Overlayed HSQC spectra of the two isoforms of glycine 42 of cytochrome b_5 as ruthenium bipyridine complex is added. Blue represents no ruthenium present. Green is 75.3 µM Ru. Red is 137.0 µM Ru. And gray is 232.2 µM Ru.
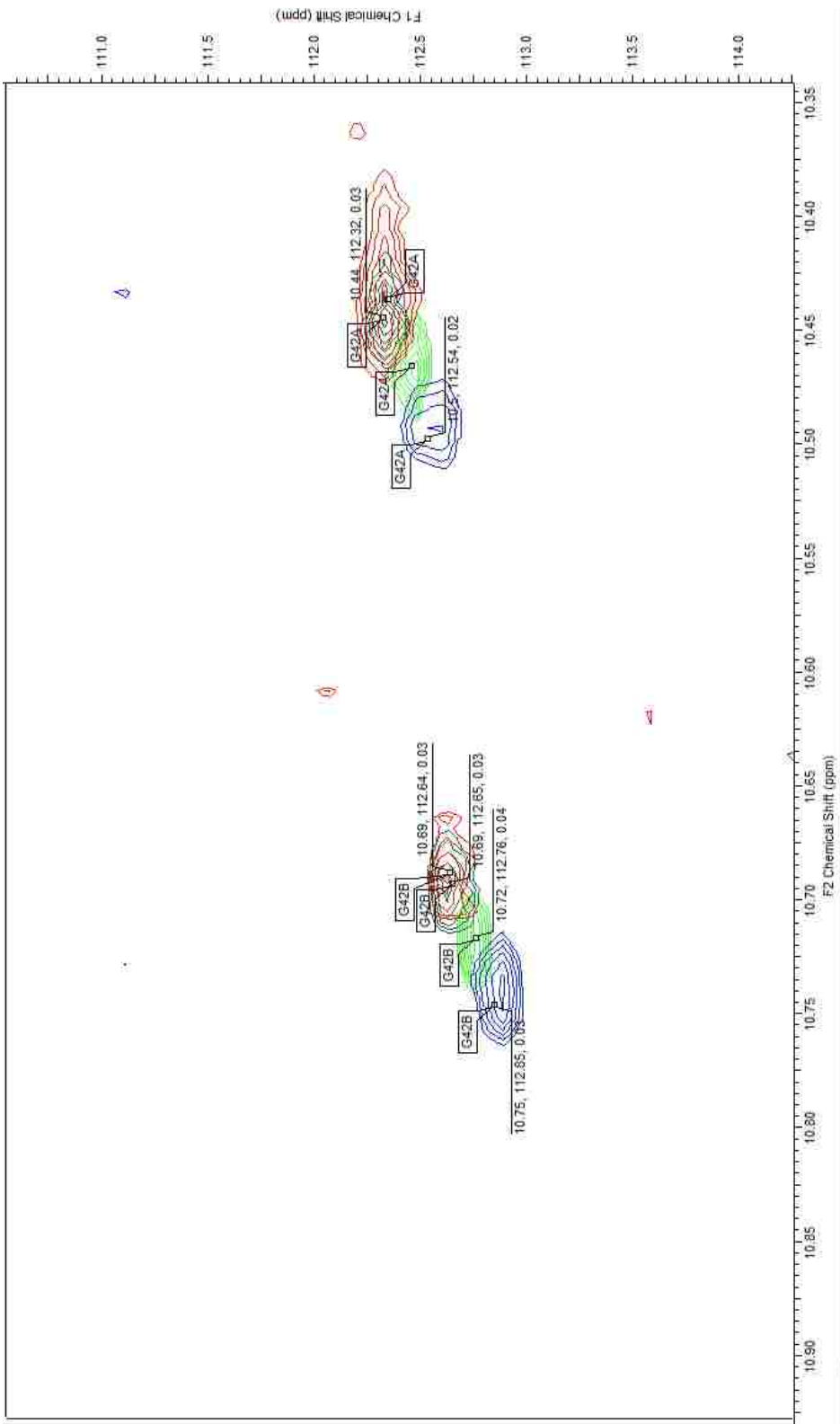
The coordinates for each peak were compared from the first spectra (0 µM Ru) and the last (232.2 µM). Perturbations were calculated as outlined above and multiplied by 100 as a visualization tool.

Resonance perturbations ranged from less than one to more than thirteen with a standard deviation of 2.05. See Figure 3-6 for histogram of all perturbations. All perturbations above two times the standard deviation, 4.10, were considered significant; all perturbations below this number were considered background. Table 3-1 shows the coordinates of each residue with significant perturbation after each addition of (Ru-bpy$_2$)$_2$-diphen, and Table 3-2 shows the perturbation of each residue after each addition. Histidine 39 ligates the iron ion of the heme, and the A and B isoforms showed an average perturbation of 3.18, which is just under the cut-off. It is included in these tables because of its importance in coordinating the iron.

Figure 3-7 shows a portion of the HSQC spectra after the final addition of (Ru-bpy$_2$)$_2$-diphen. Residues H63, G42, and V61A show significant perturbation while residues V23, S71 show very little. Peak V61B seems to have disappeared in this example. Since both isoform peaks moved in parallel in the presence of Ru bipyridine complex and in the temperature study, it is likely that V61B moved to the same position as Q13, which did not move.

Those residues with significant perturbations were highlighted on a model of microsomal rat liver cytochrome b$_5$ (PDB 1AW3). See Figure 3-8. From the figure, residues clustered around either side of the heme show the most perturbation.

Figure 3-6: Histogram of residue perturbations in the presence of 232.2 μM (Ru-bpy$_2$)$_2$-diphen
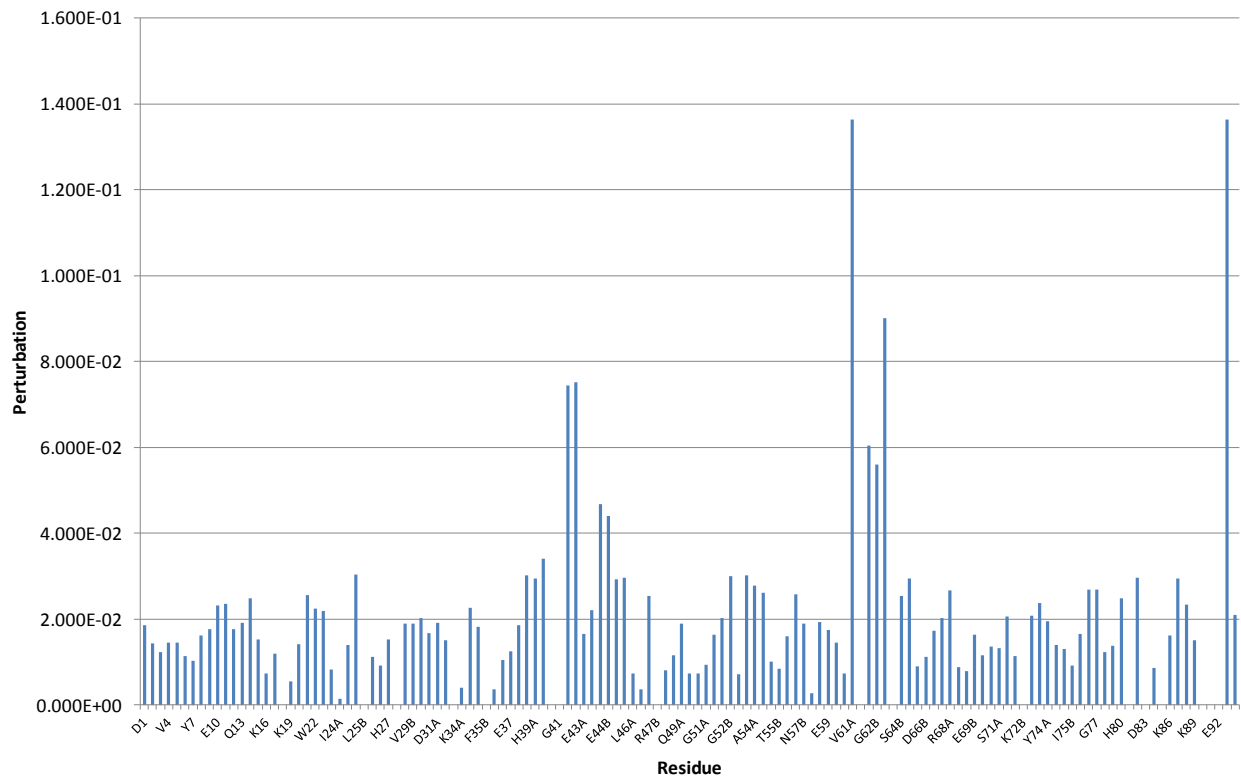
Table 3-1: Coordinates of significantly perturbed residues after each addition of [(Ru-bpy$_2$)$_2$-diphen]$^{4+}$ solution.

| | b5 conc µM | 153.00 | | 137.80 | | 125.40 | | 115.00 | | 106.30 |
| | Ru conc µM | 0.00 | | 75.30 | | 137.00 | | 188.60 | | 232.20 |
	F2	F1	F2	F1	F2	F1	F2	F1	F2	F1
H39A	8.93	120.03	8.93	120.02	8.92	119.89	8.93	119.90	8.92	119.89
H39B	8.80	119.76	8.79	119.71	8.79	119.60	8.79	119.61	8.78	119.62
G42A	10.50	112.54	10.47	112.46	10.44	112.33	10.44	112.34	10.44	112.35
G42B	10.75	112.85	10.72	112.76	10.69	112.65	10.69	112.64	10.69	112.64
E44A	9.50	124.02	9.53	124.07	9.55	124.08	9.55	124.07	9.55	124.09
E44B	9.55	124.19	9.58	124.22	9.59	124.18	9.59	124.23	9.59	124.19
V61A	8.17	114.87	8.12	114.53	8.10	114.26	8.10	114.27	8.10	114.29
G62A	8.95	109.19	8.92	109.05	8.91	108.93	8.91	108.97	8.91	108.97
G62B	8.93	108.93	8.92	108.83	8.90	108.70	8.90	108.68	8.90	108.69
H63A	11.04	119.17	11.01	119.03	10.98	118.91	10.97	118.89	10.96	118.92

Table 3-2: Perturbations of significant residues after each addition of [(Ru-bpy$_2$)$_2$-diphen]$^{4+}$ solution.

b5 conc μM	153	137.8	125.4	115	106.3
Ru conc μM	0	75.3	137	188.6	232.2
H39A	0.00	0.45	2.84	2.59	2.94
H39B	0.00	1.29	3.46	3.28	3.41
G42A	0.00	3.78	7.06	6.99	7.45
G42B	0.00	3.77	6.93	7.34	7.52
E44A	0.00	3.28	4.64	4.43	4.69
E44B	0.00	3.06	4.10	4.28	4.40
V61A	0.00	8.47	14.15	14.24	13.64
G62A	0.00	3.92	6.48	5.91	6.04
G62B	0.00	2.44	5.63	6.05	5.61
H63A	0.00	4.31	8.21	9.24	9.01

Figure 3-7: Portion of HSQC spectra of cytochrome b_5 in the presence $[(Ru\text{-}phen_2)_2\text{-}diphen]^{2+}$ (red) and without $[(Ru\text{-}phen_2)_2\text{-}diphen]^{2+}$ (blue). Peak assignments as well as three dimensional coordinates (^1H shift, ^{15}N shift, intensity) are labeled.

Figure 3-8: Solution ball and stick structure of microsomal rat liver cytochrome b$_5$ (PDB 1AW3). Residues with a perturbation from 3.0-8.0 are highlighted in yellow, and residues with perturbations from 8.1-14.0 are highlighted in green. Residues that show no perturbation are blue and the heme is red.

3.2 Isothermal Calorimetry

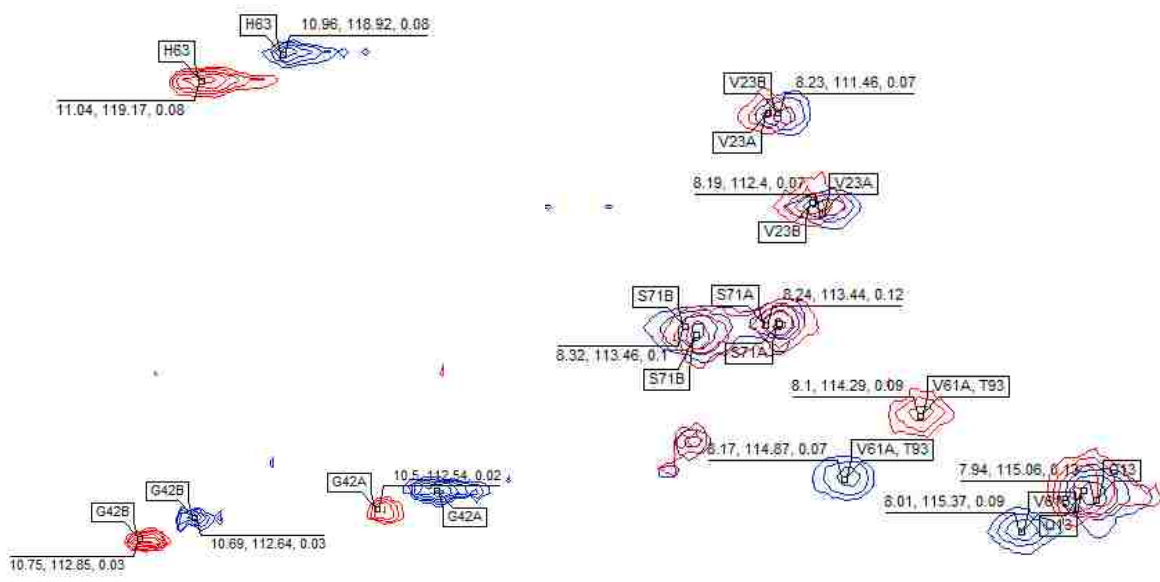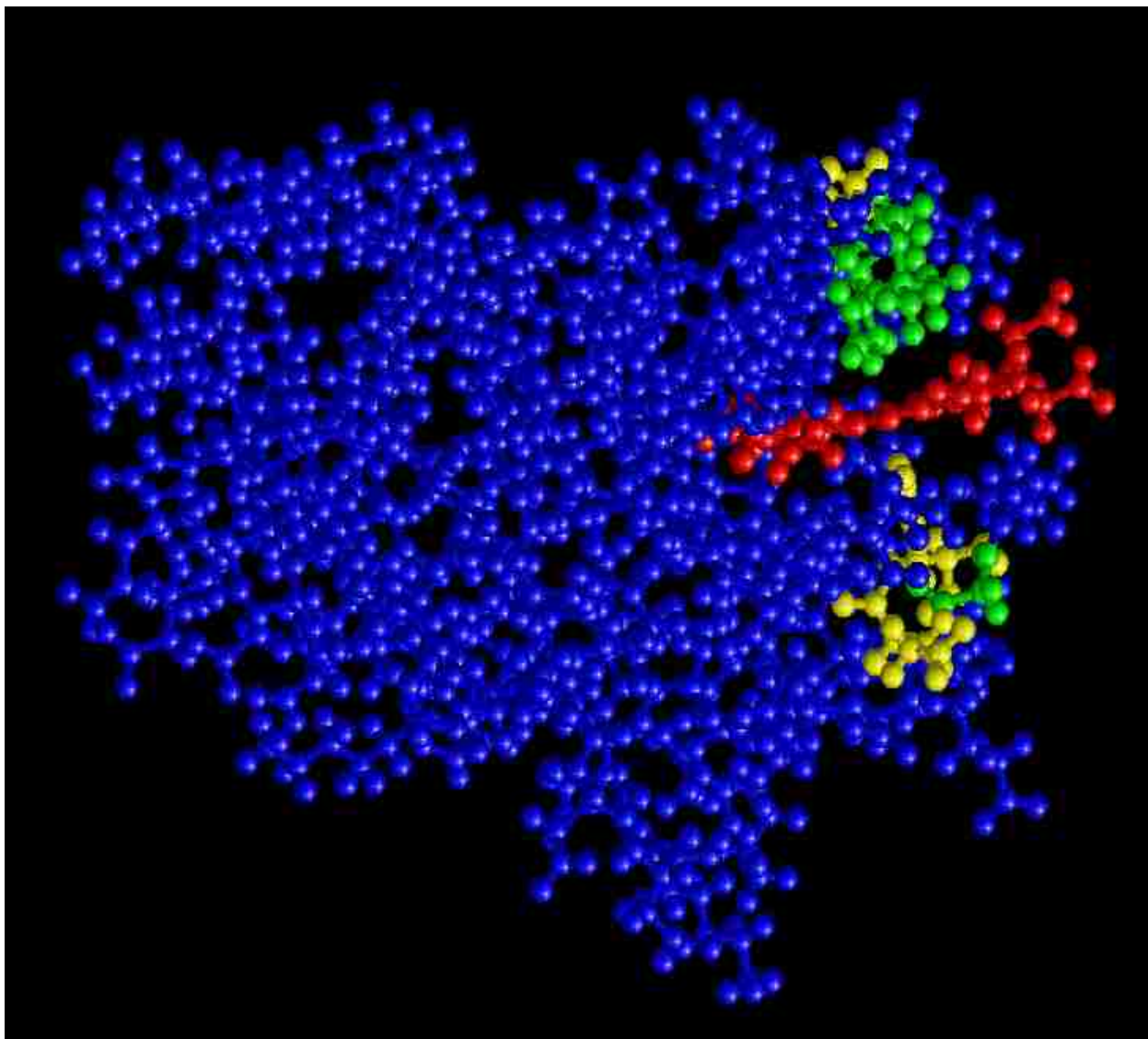Isothermal calorimetry studies were used to investigate the thermodynamic properties of cytochrome b_5 binding with the ruthenium bipyridine complex. The heat of binding was measured in as the ruthenium bipyridine complex was titrated in. Using this data and the concentrations of each solution, values for enthalpy of binding, dissociation equilibrium constant, stoichiometric ratio, and entropy of reaction were calculated.

After several trials, the data fit was poor every time which resulted in large chi squared values and error ranges. Experiments with ratio of 9.8 and 15.7:1 concentrations of ruthenium bipyridine complex to cytochrome b_5 resulted in the data never leveling off, which means saturation of the binding sites on the protein was never achieved. Saturation is critical for proper data fit. Increasing the ratio to 26.3:1 and 37.1:1 resulted in the data leveling off too quickly and increased noise, which also yields a poor fit. See figure 3-10.

Processing the data with the OneSites binding model gave stoichiometric ratios from 0.941 to 1.06, disassociation equilibrium constants K_d from 1,600 to 160,000 mM^{-1}, enthalpy of binding ΔH from +2,200 to +22,000 calories per mole, and change in entropy ΔS from 31.5 to 90.8 calories per mole per degree Kelvin. See Table 3-3 for representative calorimetry data.

3.3 Laser Flash Photolysis

The emission decay of Ru was used to determine the ratio of bound to unbound cytochrome b5 to the ruthenium complex $[(\text{Ru-phen}_2)_2\text{-diphen}]^{4+}$. The excited state lifetime of free ruthenium was measured using the emission at 600 nm. The decay of the emission at 600

Figure 3-9: Representative calorimetry data including graphs of the change in heat during the titration vs. time, graphs of total heat of each injection vs. molar ratio with trendline, and calculated thermodynamic values with statistical analysis
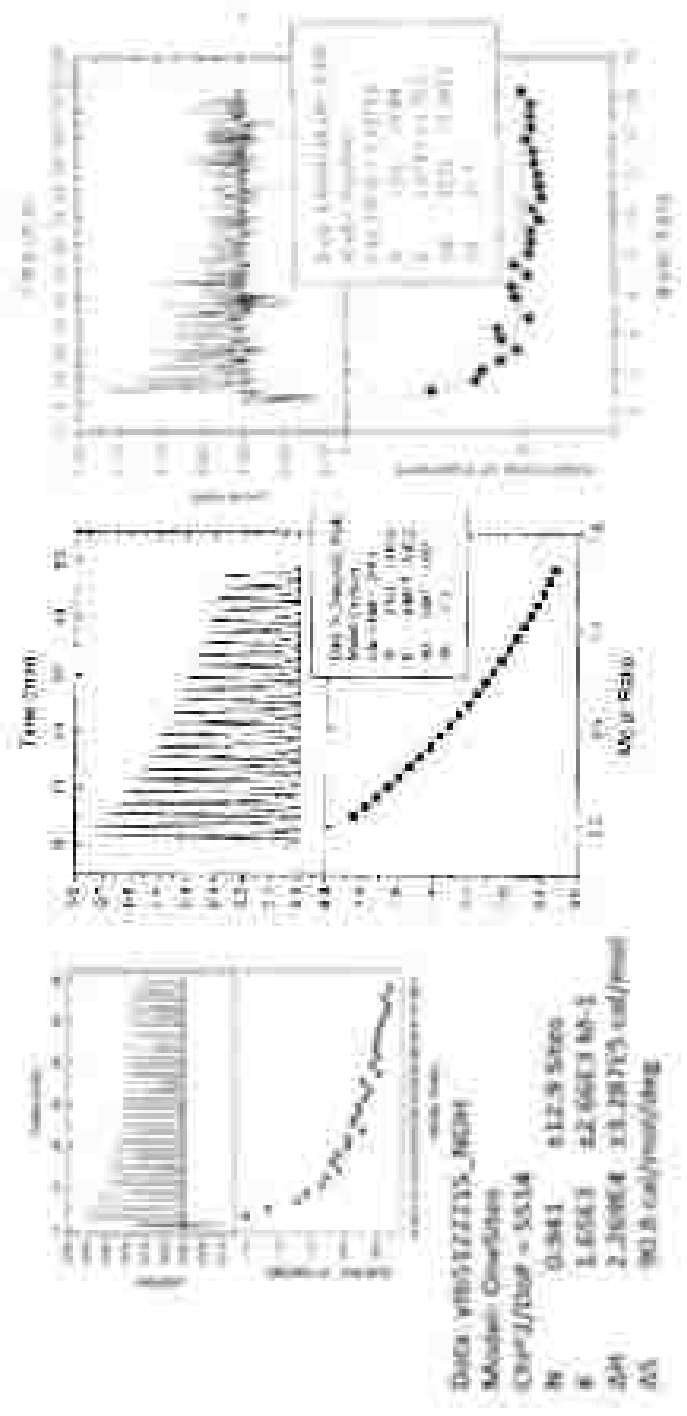
Table 3-3: Summary of data acquired with isothermal calorimetry experiments. All experiments used a stock ruthenium bipyridine complex concentration of 1 mM. Experiment 1 used a b_5 concentration of 102 μM for a Ru:b_5 ratio of 9.77 . Experiment 2 used a b_5 concentration of 63.0 μM for a ratio of 15.86. Experiment 3 used a b_5 concentration of 28.8 μM for a ratio of 37.33.

	Experiment 1	Experiment 2	Experiment 3
Stiochemtric ratio (n) Ru : protein	0.941 ± 12.9	0.951 ± 0.058	1.06 ± 0.84
Binding constant (K) mM^{-1}	1.65 ± 2.66	4.48 ± 0.58	167 ± 170
Enthalpy of binding (ΔH) cal/mol	+22690 ± 328700	+4462 ± 502	+2276 ± 2300
Entropy of reaction (ΔS) cal/mol·°K	+90.8	+31.7	+31.5

nm was best fit using a single exponential algorithm. In the presence of cytochrome b_5,

however, the decay of the excited state showed two distinctive phases. The resulting transient

shows a rapid decay of the excited state from quenching and the slower decay from unbound

ruthenium phenanthroline complex. These biphasic transients were fit with a two-exponential

algorithm. See Figure 3-10.

Comparison of the amplitudes of each phase yields a ratio of bound to unbound

ruthenium phenanthroline complex.   Table 3-4 shows the ratios and percent bound ruthenium

phenanthroline complex at varying concentrations and temperatures. Using the bound to

unbound ratio, the change in concentration can be calculated by:

$$x = \frac{\text{ratio of bound to unbound} \cdot \text{initial concentration of Ru complex}}{1 + \text{ratio}} \qquad \textbf{Equation 3-1}$$

The dissociation constant K_d can be calculated by substituting in equilibrium expression:

$$K_d = \frac{[Ru_i - x] \cdot [b_{5i} - x]}{x} \qquad \textbf{Equation 3-2}$$

The K_d values at the same temperature were averaged and a plot of the inverse of the temperature

in Kelvin vs. the natural log of the K_d values was made. See Figure 3-11. The enthalpy of

dissociation can be calculated from the plot as:

$$\Delta H° = \text{-slope} / R \qquad \textbf{Equation 3-3}$$

And the entropy of dissociation can be calculated as:

$$\Delta S° = \text{intercept} / R \qquad \textbf{Equation 3-4}$$

From the graph, the slope is 463.42. Multiplying by -1 and dividing by R (1.987 cal/ mol · K)

yields a $\Delta H°$ of dissociation = -200 ± 200 cal / mol after applying the standard error of slope/R.

The intercept is -11.6. Dividing by R gives a $\Delta S° = $ -6 ± 1 with the standard error slope/R.

Figure 3-10: Typical fit of biphasic absorbance decay of ruthenium phenanthroline complex (6.2 µM) with cytochrome b$_5$ (22.6 µM) at 25˚C.

97
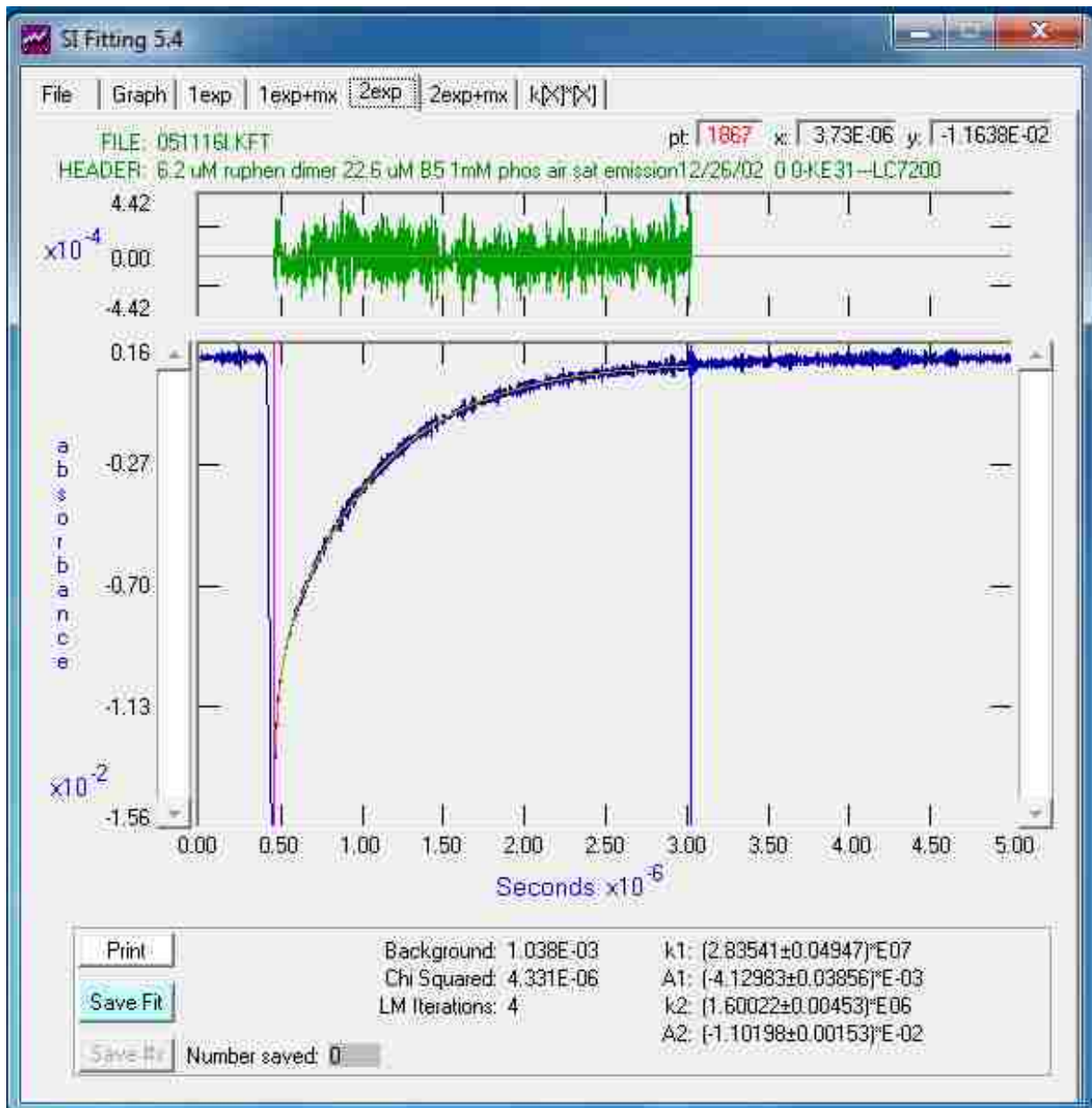
Table 3-4: Table of dissociation constants, ratios, and percent bound ruthenium phenanthroline complex with cytochrome b_5 with varying temperatures andconcentrations acquired using laser flash photolysis and excited state lifetime analysis.

Ru conc μM	b₅ conc μM	Temp K	ratio bound to unbound	% bound	Δ conc μM	K_d μM
6.2	22.6	294	0.473	32.11	1.99	43.57
6.2	22.6	294	0.434	30.27	1.88	47.73
6.2	22.6	282	0.453	31.19	1.93	45.59
6.2	22.6	282	0.413	29.25	1.81	50.28
6.2	22.6	302	0.470	31.97	1.98	43.87
5.2	38.9	294	0.913	47.73	2.48	39.87

Figure 3-11: Graph of the inverse of the temperature 1/T vs. ln Kd for the dissociation reaction:

$[(Ru\text{-}phen_2)_2\text{-}diphen]^{2+}\text{--cyt } b_5 \rightleftharpoons [(Ru\text{-}phen_2)_2\text{-}diphen]^{2+} + \text{cyt } b_5$

1/T vs. ln K$_d$

y = 463.42x - 11.6

ln K$_d$

1/T
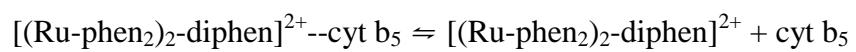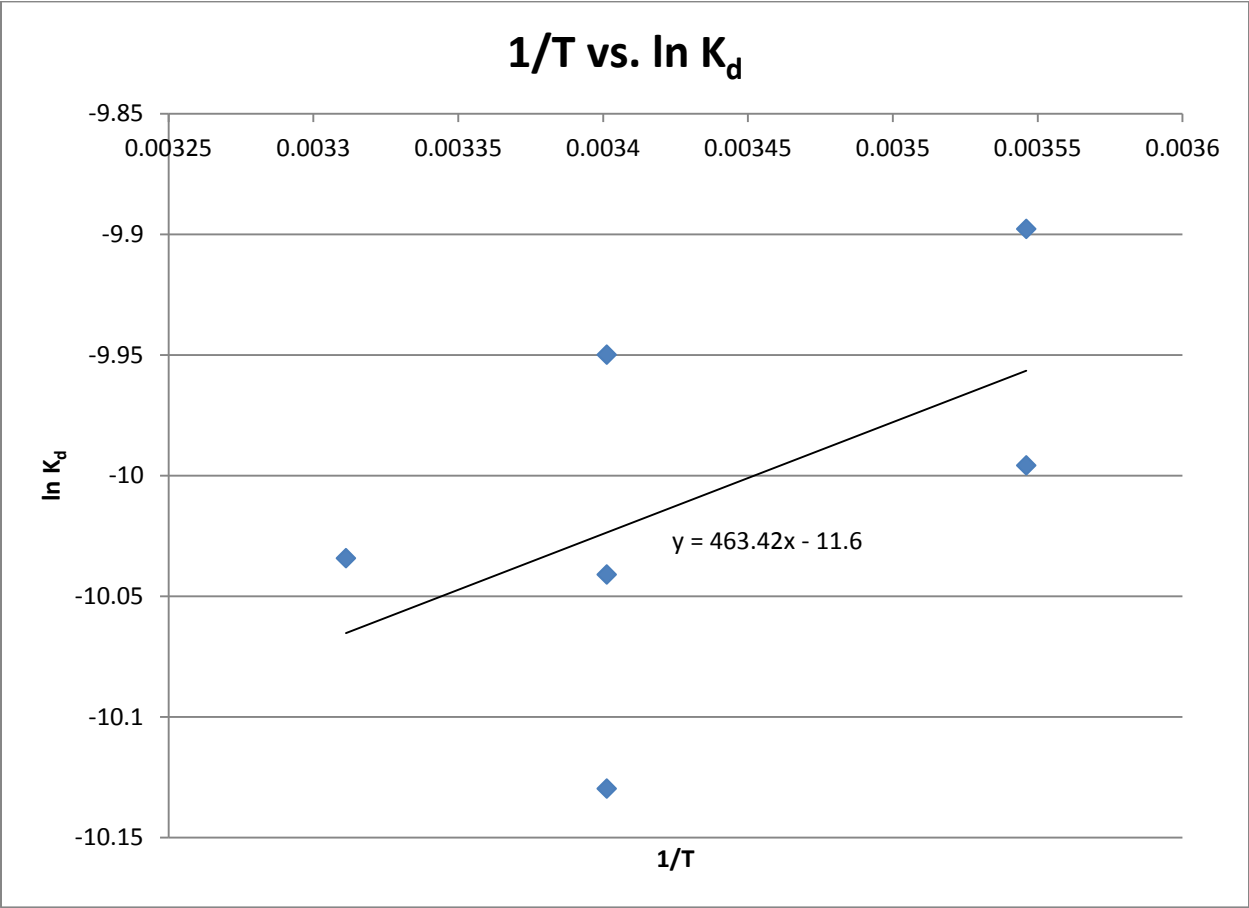
Chapter 4 – Discussion

4.1 – Significance

The redox properties of the excited state of ruthenium(II) bipyridine complexes make them ideal candidates for the study of electron transfer reactions in general. The long lived excited state provides a means of generating sufficient quantities of reactive intermediates in experiments such as laser flash photolysis to ensure high signal to noise ratios and ultimately high quality kinetic data. Covalent binding of the ruthenium complex to a metalloprotein was an obvious first step and early investigators took this step which proved to be extremely fruitful. The early work was done with relatively small proteins that were sufficiently robust to allow the chemistry required to produce a covalent bond. Application to much larger proteins such as those found in the electron transport chain did not appear to be practical. Fortunately a remarkable discovery was made by Nilsson in (1992). Nilsson showed that it was possible to use ruthenium trisbipyridine in solution to transfer an electron to cytochrome c oxidase. This was a remarkable finding and strongly suggested that the ruthenium complex bound to an area very near to Cu_A. A strong electrostatic interaction was presumed. Subsequent work by Millett et al. showed that complexes with higher charge were able to provide better signals with significantly smaller concentrations of ruthenium complex.

Tracey Jackson (2001) did an in depth study and as mentioned in the introduction found in a model study with cytochrome b_5 that binding of complexes with the same charge was very similar and independent of the structure of the complex. He also found that binding affinity increased with the overall charge of the complex. His data was obtained by examining the

excited state decay kinetics in the presence of increasing amounts of cytochrome b5. The excited

state kinetics was determined by monitoring the emission from the ruthenium complexes as a

function of time. In all cases biphasic kinetics were observed at high concentrations of protein.

The observations were interpreted in terms of a two reaction model. In one reaction the

ruthenium complex was bound to the protein resulting in very fast quenching and in the second

reaction the ruthenium complex simply decayed naturally as if in absence of protein. The latter

was easily verified by examining the decay kinetics in the absence of protein.

At this point it is reasonable to assume that the ruthenium complex must interact with the

protein close to the heme because the reaction must take place within the life time of the excited

state. The experimental data as well as many other experiments with excited states supports the

idea that diffusion of the complex while in the excited state will not lead to any significant

quenching by the protein.

At the beginning of the project described in this dissertation the question was asked

whether or not additional information about the binding could be obtained. Specifically, could

the binding domain be identified? Recent advances in NMR technology have made many

experiments routine that were previously not workable because of the amounts of material

required. ^{15}N HSQC for example can be done with extremely small amounts of protein and it is

one of the experiments of choice identifying binding domains. The work described in this

dissertation was focused primarily on this experiment. In addition, several attempts were made

to obtain thermodynamic data related to the binding.

4.2 – NMR Analysis

It has long been speculated that ruthenium complexes binds at the protein's natural substrate binding site near the heme during laser flash photolysis experiments (Guiles et al., 1993; Durham et al., 1997). Proximity from the ruthenium atom of the bipyridine complex to the iron atom of the heme would provide the lowest energy pathway for electron transfer to occur. It has also been shown that binding affinity increases with overall charge of the complex (Davidson, 2000). This is likely due to the preponderance of negatively charged residues in the protein's natural substrate binding site. But there has never been evidence that proves conclusively that this is the case.

The NMR data presented in this study demonstrates that these speculations are likely correct. The residues most perturbed in the presence of the ruthenium bipyridine complex fall right on either side of the heme cleft of the protein. It has been shown that the heme proprionate groups play a role in cytochrome b_5 (Gray et al., 2003). This technique only reveals distortion of the protein's backbone. It does not rule out interaction of ruthenium complexes with the heme proprionates.

Figure 4-1 shows a plot of the perturbations of each residue vs. the molar ratio of Ru dimer to cytochrome b_5. Each line levels off around a molar ratio of 1. This is evidence that the binding stoichiometry is 1:1. The graph also includes a theoretical fit of the data using a hypothetical K_d of 5 µM. Valine 61 is the most perturbed residue. It is reasonable to assume that as the bipyridine complex binds near this residue, its perturbation is propagated through the backbone affecting other residues proportionately. It is interesting to note that there was no difference in binding between isoforms.

Figure 4-1: Plot of NMR perturbation vs. molar ratio of Ru/b$_5$. Included is a theoretical fit of the data using a hypothetical Kd of 5 µM.
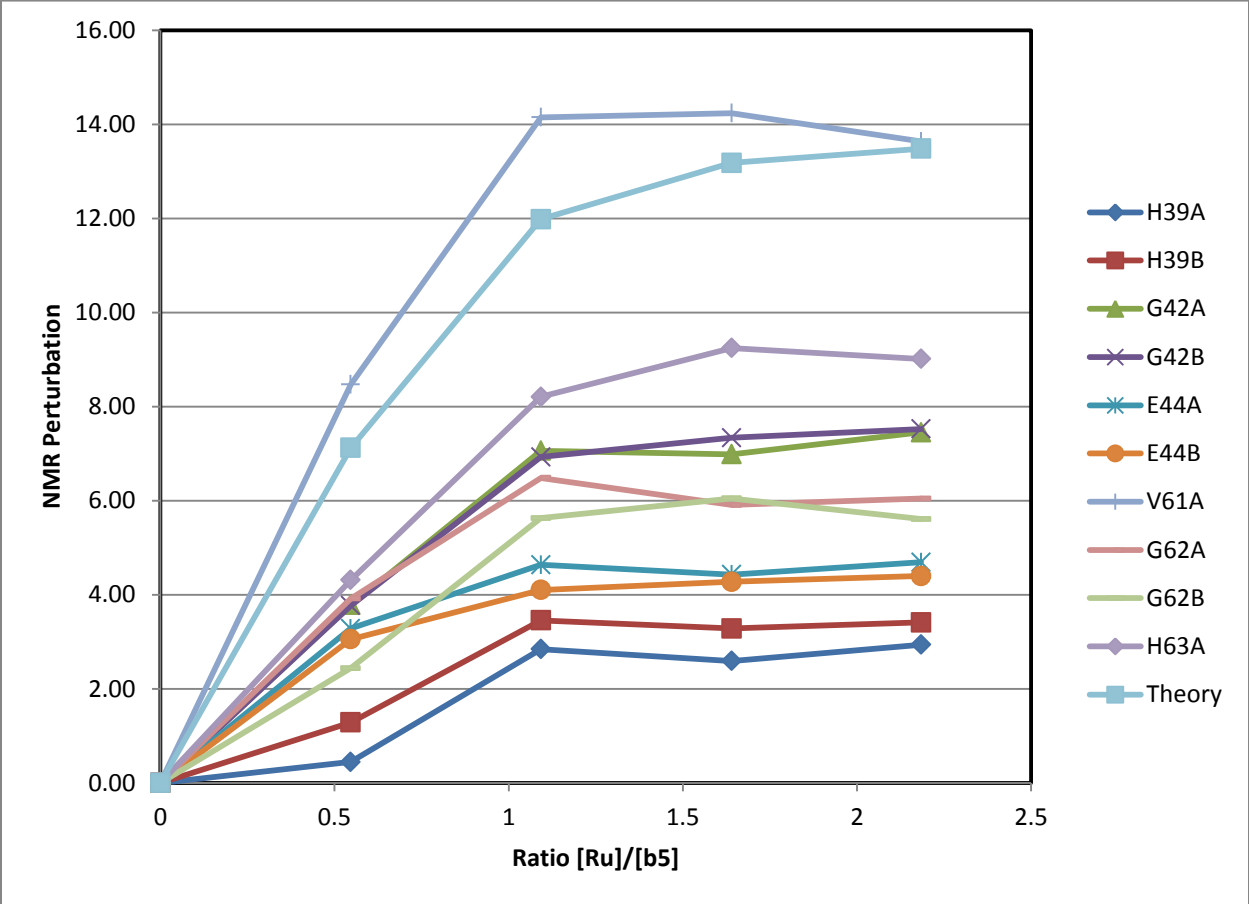
Figure 4-2 shows a backbone diagram of cytochrome b5 showing charged residues and the residues that show significant shifts in resonances energies in the HSQC spectra upon the addition of the ruthenium bipyridine dimer.

Cytochrome b_5 has been shown to bind to substrates in multiple orientations and sites (Volkov et al., 2005). It is likely that ruthenium dimer complexes also bind in a similar dynamic manner. Resonances in the spectra represent an average of all the species in solution over time. The timescale of the HSQC experiment is above the rapid exchange limit of the binding reaction.

4.3 – Isothermal Calorimetry Analysis

Previous studies utilizing laser flash photolysis techniques have calculated the dissociation constant K_d for ruthenium complexes with an overall charge of +4 of 8.8 µM in 1 mM phosphate buffer (Jackson, 2001). Taking the reciprocal and converting to mM^{-1} gives a binding constant K_a of 113 mM-1. The present work using ITC found a K_a between 1 and 200 mM^{-1} in 10 mM phosphate buffer. While there is a substantial error range with this figure, the previous determined values do fall within this range even if the ionic strength differs by a factor of ten.

The value for the enthalpy of binding ΔH for ruthenium dimer complexes has not been determined previously using other methods. But the values from these experiments from +2,200 to +22,000 calories per mole. This is not consistent with favorable binding equilibrium constant. Previous research has evaluated the ΔH for the binding of cytochrome b_5 to cytochrome c using similar techniques in 2 mM phosphate buffer around 1000 cal/mole (Mclean et al., 1995), which is comparable.

Figure 4-2: Solution backbone structure of microsomal rat liver cytochrome b_5 (PDB 1AW3). Residues with a significant perturbation are in green and acidic residues are in red. The coordinating histidines are in purple.
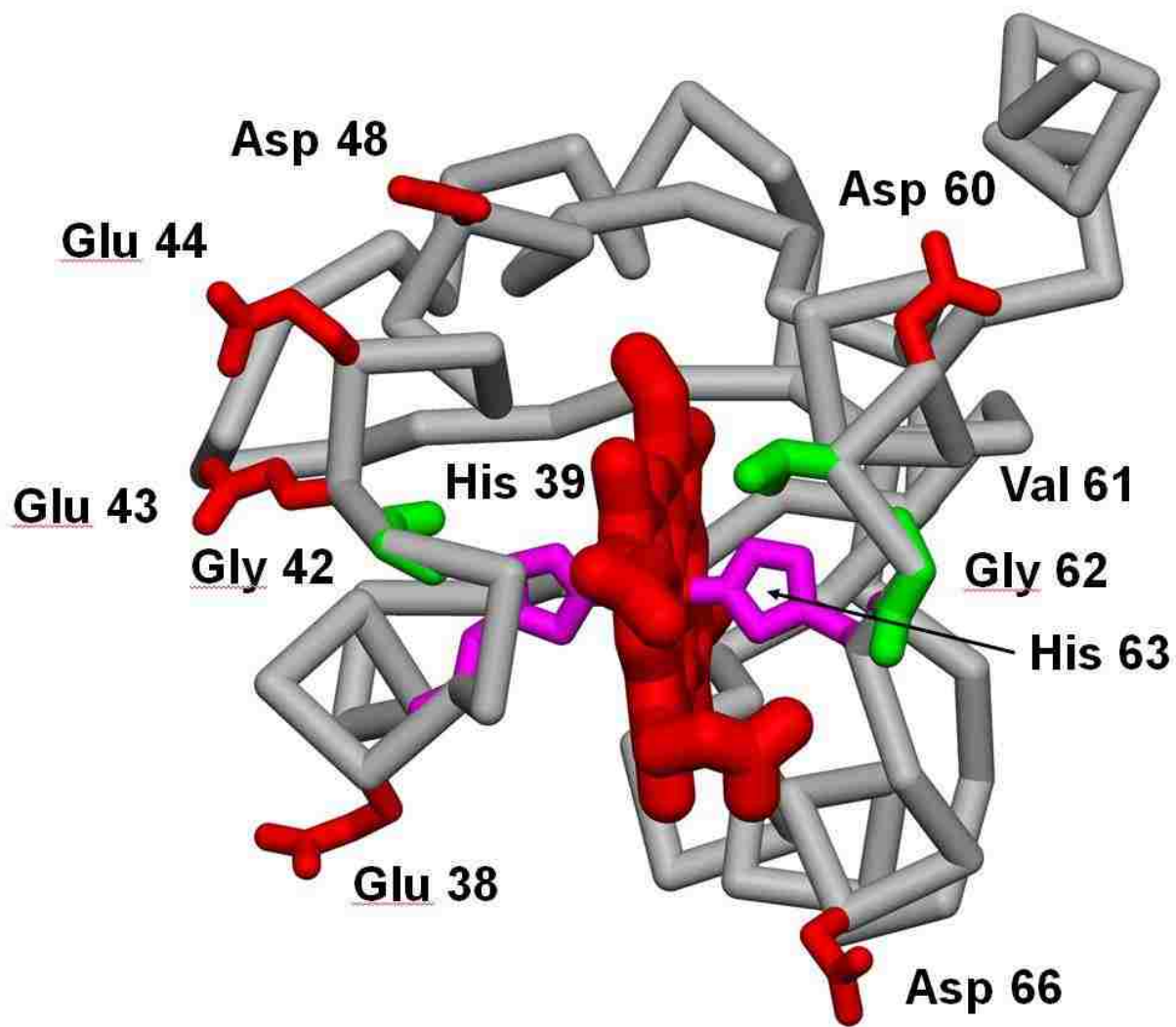
The values for the entropy of the binding reaction ranged from +31 to +91 cal/mol·K. The entropy of interaction between the Ru bipyridine complex dimer has not been evaluated previously, but researchers determined the entropy of binding for cytrochrome b_5 and cytochrome c in 2 mM phosphate buffer to be about 33.9 cal/mol·K (Mclean et al., 1995). This number is also comparable despite the difference in ionic strength. The large positive values of entropy indicate that the binding is entropy controlled, i.e, the entropy component of the free energy is much larger than the small enthalpy of reaction.

Because the data was a poor fit, the error range for the stiochiometric binding ratio is large. But all experiments in this work determined a protein to complex binding ratios ranging from 0.941 to 1.06 with an average of 0.984. While this data appears to support the NMR data indicating a 1:1 binding ratio, the scattered nature of the data makes all values determined by these experiments suspect.

4.4 – Laser Flash Photolysis Analysis

New data points for $[(Ru-diphen_2)_2-diphen]^{4+}$ were added to a plot of previously determined values for fraction of ruthenium complex bound to cytochrome b_5 (Figure 4-3) (Jackson, 2001). The points fall in between the trend for other Ru complexes with an overall charge of +4 and $[Ru(bpy)_3]^{2+}$. See Figure 1-7.

The data for fraction of the phenanthroline complex bound was used to calculate the value for the dissociation constant K_d (Table 3-3). The average K_d value for all determinations was found to be 43.7 μM at 25 °C, which is higher than the Tracey Jackson's results of 8.8 μM for compounds with an overall charge of +4. This also lends evidence that the dimer with its more sterically shielded positive charge binds less tightly.

Figure 4-3: Graph of fraction of phenanthroline complex bound to cytochrome b_5 vs. the concentration of cytochrome b_5 from Tracey Jackson's work (2001). New data points representing $[(Ru-diphen_2)_2-diphen]^{4+}$ arein red.
Jackson, Tracey (2001) "Electrostatically bound metal complexes for the study of electron transfer in metalloproteins" Dissertation, University of Arkansas, Fayetteville, AR
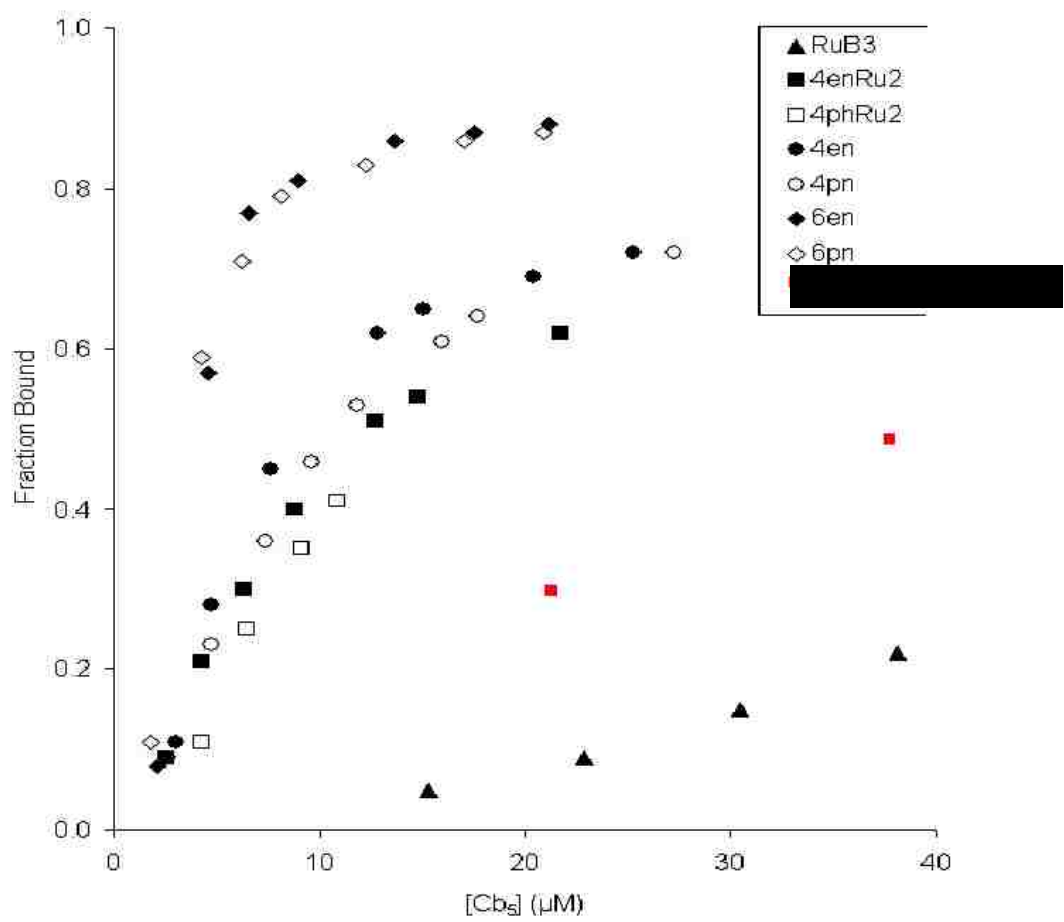
The inverse temperature 1/T was plotted vs. the natural log of the dissociation constant K_d. From the slope and intercept of this line, the values for the enthalpy of dissociation ΔH and entropy of dissociation ΔS were determined to be -233 cal/mol and -5.84 cal/mol·K respectively (Figure 3-11). The corresponding values for the association reaction gives the enthalpy and entropy of binding equal to $+200 \pm 200$ cal/mol and $+6 \pm$ cal/mol·K. Again we see a reaction that is entropy controlled. These values are lower than the values from the calorimetry experiments, ΔH of about +3000 cal/mol and ΔS of about +30 cal/mol·K likely because of the difference in ionic strength.

4.5 – Conclusions

Photoreactive ruthenium complexes to study the kinetics of electron transfer of proteins have been in use for decades (Isied et al., 1984; Tollin et al., 1991; Peterson-Kennedy et al., 1985; Nocera et al., 1984). It has always been speculated that complexes bind near the heme or the electron transfer reaction would not occur. But there has never been any data to show that is the case. NMR studies in this body of this work supports the long believed model of a ruthenium dimer binding dynamically near the heme. The thermodynamic properties of the binding between Ru dimer complexes to cytochrome b_5 had not been explored previously. This study confirms that the binding reaction is energetically favorable, and that equilibrium favors the bound state, and the binding stoichiometry is indeed 1:1. These insights will help with the design of future photoreactive complexes for the study of electron transfer reactions in metalloproteins.

Bibliography

Altuve, Adriana; Silchenko, Svetlana; Lee, Kyung-Hoon; Kuczera, Krzysztof; Terzyan, Simon; Zhang, Xuejun; Benson, David R.; Rivera, Mario (2001) "Probing the Differences between Rat Liver Outer Mitochondrial Membrane Cytochrome b5 and Microsomal Cytochromes b5". Biochemistry 40, 9469-9483

Argos, P., Mathews, F. (1975) "The Structure of Ferrocytochrome b, at 2.8 A Resolution" Journal of Biological Chemistry 250: 747-751

Arnesano, F., Banci, L., Bertini, I., Felli, I.C. (1998) "The solution structure of oxidized rat microsomal cytochrome b5" Biochemistry 37: 173-184

Beck von Bodman S; Schuler M A; Jollie D R; Sligar S G (1986) "Synthesis, bacterial expression, and mutagenesis of the gene coding for mammalian cytochrome b5" Proc Natl Acad Sci USA, 83(24) 9443-9447

Beratan, D. N.; Betts, J. N.; Onuchic, J. N. (1991) "Protein electron transfer rates set by the bridging secondary and tertiary structure" Science 252, 1285-1288.

Berry, E. A., Guergova-Kuras, M., Huang, L. & Crofts, A. R. (2000) "Structure and Function of Cytochrome bc Complexes." Annu. Rev. Biochem. 69, 1005-1075

Bodenhausen, G.; Ruben, D.J. (1980). "Natural abundance nitrogen-15 NMR by enhanced heteronuclear spectroscopy". Chemical Physics Letters 69 (1): 185–189

Cavanagh, J., W. Fairbrother, A.G. Palmer III and N.J. Skleton (2007) "Protein NMR Spectroscopy – Principles and Practice" 2nd Ed. Academic Press

Chudaev, M.V. A.A. Gilep, S.A. Usanov, (2001) "Site-directed mutagenesis of cytochrome b5 for studies of its interaction with cytochrome P450", Biochemistry (Moscow) 66 667–681.

Cordes, M., and Giese, B. (2009) "Electron transfer in peptides and proteins", Chem. Soc. Rev. 38(4), 892-901

Davidson, V. L. (2000) "What controls the rates of interprotein electron-transfer reactions", Ace. Chem. Res. 33(2), 87-93

do Nascimento T.S., Pereira R.O., de Mello H.L., Costa J. (2008) "Methemoglobinemia: from diagnosis to treatment" Revista Brasileira de Anestesiologia. 58, 657-664

Durham, B., Millett, F. (1997) "Ruthenium (II) Polypyridine Complexes and the Electron-Transfer Reactions of Metalloproteins" Journal of Chemical Education 74: 636-651

Durham, B.; Pan, L. P.; Long, J. E.; Millett, F. (1989) "Photoinduced electron-transfer kinetics of singly labeled ruthenium bis(bipyridine) dicarboxybipyridine cytochrome c derivatives." Biochemistry (N.Y.), 28, 8659-8665

Durham, Bill; Millett, Frank (1997) "Ruthenium II Polypyridine Complexes and the Electron-Transfer Reactions of Metalloproteins" Journal of Chemical Education, 74 (6) 636-640.

Eley, C.G.S. and Moore, G.R. (1983) "1H NMR Investigation of the interaction between cytochrome c and cytochrome b5" Biochem. Journal 215, 11–21.

Funk, Walter D.; Lo, Terence P.; Mauk, Marcia R.; Brayer, Gary D.; MacGillivray, Ross T. A.; Mauk, A. Grant (1990) "Mutagenic, electrochemical, and crystallographic investigation of the cytochrome b5 oxidation-reduction equilibrium: involvement of asparagine-57, serine-64, and heme propionate-7" Biochemistry 29, 5500-5509

Gomathi, L., (1996) "Elucidation of secondary structures of peptides using high resolution NMR." Current Science, 71, 553-567

Gray, H. B., and Winkler, J. R. (2003) "Electron tunneling through proteins", Q. Rev. Biophys. 36(3), 341-372.

Grigorieff, N. (1998). "Three-dimensional structure of bovine NADH:ubiquinone oxidoreductase (complex I) at 22 å in ice" J. Mol. Biol. 277 , 1033-1046.

Guiles, R. D. ,Vladimir J. Basus, Siddhartha Sarma, Swati Malpure, Kristine M. Fox, Irwin D. Kuntz and Lucy Waskel. (1993) "Novel Heteronuclear Methods of Assignment Transfer from a Diamagnetic to a Paramagnetic Protein: Application to Rat Cytochrome b5" Biochemistry 32, 8329-8340

Havens, J. (2010) "Ruthenium flash initiated studies of electron transfer between cytochrome c and the b hemes of cytochrome b5 and sulfite oxidase, and the electron transfer within cytochrome bc1" Dissertation, University of Arkansas, Fayetteville, AR

Hultquist, Donald E.; Sannes, Lucy Jean; Juckett, David A (1984) "Catalysis of methemoglobin reduction" Current Topics in Cellular Regulation 24, 287-300

Imai, Yoshio; Sato, Ryo (1977) "The roles of cytochrome b5 in a reconstituted N-demethylase system containing cytochrome P-450" Biochemical and Biophysical Research Communications 75, 420-426

Isied, S. S.; Kuehn, C.; Worosila, G. (1984) "Ruthenium-modified cytochrome c: temperature dependence of the rate of intramolecular electron transfer" J. Am. Chem. Soc., 106, 1722–1726.

Isied, S. S.; Worosila, G.; Atherton, S. J. (1982) "Electron transfer across polypeptides. 4. Intramolecular electron transfer from ruthenium(II) to iron(III) in histidine-33-modified horse heart cytochrome c" J. Am. Chem. Soc. 104, 7659–7661.

Iwata S, Lee JW, Okada K, Lee JK, Iwata M, Rasmussen B, Link TA, Ramaswamy S, Jap BK (1998). "Complete structure of the 11-subunit bovine mitochondrial cytochrome bc1 complex". Science 281, 64–71

Jackson, Tracey (2001) "Electrostatically bound metal complexes for the study of electron transfer in metalloproteins" Dissertation, University of Arkansas, Fayetteville, AR

Keller, Regula; Groudinsky, Olga; Wuethrich, Kurt (1976) "Contact-shifted resonances in the proton NMR spectra of cytochrome b5. Resonance identification and spin density distribution in the heme group" Biochimica et Biophysica Acta, Protein Structure 427, 497-511

La Mar, Gerd N.; Burns, Phillip D.; Jackson, J. Timothy; Smith, Kevin M.; Langry, Kevin C.; Strittmatter, Philipp (1981) "Proton magnetic resonance determination of the relative heme orientations in disordered native and reconstituted ferricytochrome b5. Assignment of heme resonances by deuterium labeling" Journal of Biological Chemistry 256, 6075-6079

Lee, Kang-Bong; McLachlan, Stuart J.; La Mar, Gerd N (1994) "Hydrogen isotope effects on the proton nuclear magnetic resonance spectrum of bovine ferricytochrome b5: Axial hydrogen bonding involving the axial His-39 imidazole ligand" Biochimica et Biophysica Acta, Protein Structure and Molecular Enzymology 1208 22-30

Matheson, I. B. C. (1987). "The Method of Successive Integration: a General Technique for Recasting Kinetic Equations in a Readily Soluble Form Which Is Linear in the Coefficients and Sufficiently Rapid for Real Time Instrumental Use" Instrumentation Science & Technology 16, 345–373.

Mathews, F. Scott (1985) "The structure, function and evolution of cytochromes" Progress in Biophysics & Molecular Biology 45, 1-56

Matlib, M., O'Brien, P. (1976) "Properties of rat liver mitochondria with intermembrane cytochrome c." Archives of Biochemistry and Biophysics, 173, 27-33

Mauk, M.R., Mauk, A.G., Weber, P.C., and Matthew, J.B. (1986). "Electrostatic analysis of the interaction of cytochrome c with native and dimethyl ester heme substituted cytochrome b5." Biochemistry 25, 7085–7091.

Mauk, M.R., Reid, L.S., and Mauk, A.G. (1982) "Spectrophotometric analysis of the interaction between cytochrome b5 and cytochrome c." Biochemistry 21, 1843–1846

McIntosh L.P., Griffey, R.H., Muchmore D.C., Nielson, C.P., Redfield, A.G., and Dahlquist, F.W. (1987) "Proton NMR measurements of bacteriophage T4 lysozyme aided by 15N isotopic

labeling: structural and dynamic studies of larger proteins." Proc Natl Acad Sci USA 84(5): 1244–1248

Mclean, M A, Sligar, S G, (1995) "Thermodynamic characterization of the interaction between cytochrome b5 and cytochrome c." Biochemical and Biophysical Research Communications 215, 316-320

Millett, Francis; Havens, Jeffrey; Rajagukguk, Sany; Durham, Bill (2013) "Design and use of photoactive ruthenium complexes to study electron transfer within cytochrome bc1 and from cytochrome bc1 to cytochrome c" Biochimica et Biophysica Acta, Bioenergetics , 1827, (11-12), 1309-1319

Miura, R., Sugiyama, T., Akasako, K., and Yamano, T. 1980. An NMR study on the interaction between cytochrome b5 and cytochrome c. Biochem. Int.1: 532–538.

Neidhardt FC, Bloch PL, Smith DF. (1974) "Culture medium for enterobacteria" Journal of Bacteriology 119(3), 736-47.

Ng, S., Smith, M.B., Smith, H.T., and Millett, F. (1977) "Effect of modification of individual cytochrome c lysines of the reaction with cytochrome b5." Biochemistry 16: 4975–4978.

Nilsson, T. (1992) "Photoinduced electron transfer from tris(2,2'-bipyridyl)ruthenium to cytochrome c oxidase" Proceedings of the National Academy of Sciences USA 89, 6497-6501

Njabon, Roland Ngebichie. (2013) "An investigation of the electronic coupling in some dimeric ruthenium (II) polyridine complexes" Dissertation, University of Arkansas, Fayetteville, AR

Nocera, D. G.; Winkler, J. R.; Yocum, K. M.; Bordignon, E.; Gray, H. B. (1984) "Kinetics of intermolecular and intramolecular electron transfer from ruthenium(II) complexes to ferricytochrome c" J. Am. Chem. Soc., 106, 5145–5150.

Northrup, S.H., Thomasson, K.A., Miller, C.M., Barker, P.D., Eltis, L.D., Guillemette, J.G., Inglis, S.C., and Mauk, A.G. (1993). "Effects of charged amino acid mutations on the bimolecular kinetics of reduction of yeast iso-1-ferricytochrome c by bovine ferrocytochrome b5." Biochemistry 32, 6613–6623.

Ozols J (1989) "Structure of cytochrome b5 and its topology in the microsomal membrane." Biochim. Biophys. Acta 997 (1-2) 121–30

Peterson-Kennedy, S. E.; McGourty, J. L.; Ho, P. S.; Sutoris, C. J.; Liang, N.; Zemel, H.; Margoliash, E.; Hoffmann, B. M. (1985) "Long-Range Electron Transfer at Fixed and Known Distance within Protein Complexes" Coord. Chem. Rev., 64, 125–133.

Puckett, Latisha (2015) "Photochemistry of a Series of Weakly Coupled Dinuclear Ruthenium(II) Complexes" Dissertation, University of Arkansas, Fayetteville, AR

Raven, P. H., and G. B. Johnson. (1986). Biology. 2nd ed. St. Louis, Mo.: Times Mirror/Mosby College.

Regan, J. J.; Risser, S. M.; Beratan, D. N., Onuchic, J. N., (1993) "Protein electron transport: single versus multiple pathways" J. Phys. Chem., 97, 13083-13088

Reid, L.S., Mauk, M.R., and Mauk, A.G. (1984). "Role of heme propionate groups in cytochrome b5 electron transfer." J. Am. Chem. Soc. 106, 2182–2185.

Rodgers, K.K. and Sligar, S.G. (1991) "Mapping electrostatic interactions in macromolecular associations." J. Mol. Biol. 221, 1453–1460.

Rodgers, K.K., Pochapsky, T.C., and Sligar, S.G. (1988). "Probing the mechanism of macromolecular recognition: The cytochrome b5 - cytochrome c complex." Science 240, 1657–1659.

Rodgers, Karla K.; Pochapsky, Thomas C.; Sligar, Stephen G (1988) "Probing the mechanisms of macromolecular recognition: the cytochrome b5-cytochrome c complex" Science 240, 1657-1659

Salemme F. (1976) "An Hypothetical Structure for an Intermolecular Electron Transfer Complex of Cytochromes c and b5" Journal of Molecular Biology 102 : 563-568

Sarma, Siddhartha; DiGate, Russell J.; Banville, Debra L.; Guiles, R. D. (1996) "1H, 13C and 15N NMR assignments and secondary structure of the paramagnetic form of rat cytochrome b5" Journal of Biomolecular NMR 8, 171-183

Smith, M.B., Stoneheurner, J., Ahmed, A.Q.J., Staudenmeyer, N., and Millett, F. 1980. "Use of specific trifluoroacetylation of lysine residues in cytochrome c to study the reaction with cytochrome b5, cytochrome c1, and cytochrome oxidase". Biochim. Biophys. Acta 592, 303–313

Stoneheurner, J., Williams, J.B., and Millett, F. (1979). "Interaction between cytochrome c and cytochrome b5". Biochemistry 18, 5422–5427.

Strittmatter, P.; Spatz, L.; Corcoran, D.; Rogers, M. J.; Setlow, B.; Redline, R (1974) "Purification and properties of rat liver microsomal stearyl coenzyme A desaturase" Proc. Natl. Acad. Sci. USA 71 4565-4569

Sun F, Huo X, Zhai Y, Wang A, Xu J, Su D, et al. (2005). "Crystal structure of mitochondrial respiratory membrane protein complex II.". Cell 121 1043–57.

Takano, T., Kallai, O.B., Swanson, R., and Dickerson, R.E. (1973) "The structure of ferrocytochrome c at 2.45 Å resolution." J. Biol. Chem. 248: 5234–5246.

Tollin, G.; Hazzard, J. T. (1991) "Intra- and intermolecular electron transfer processes in redox proteins" Arch. Biochem. Biophys. 287, 1–7.

Volkov, A. (2005) "The orientations of cytochrome c in the highly dynamic complex with cytochrome b5 visualized by NMR and docking using HADDOCK" Protein Science 14, 799–811

Wang,W.H, J.X. Lu, P. Yao, Y. Xie, Z.X. Huang, (2003) "The distinct heme coordination environments and heme-binding stabilities of His39Ser and His39Cys mutants of cytochrome b5, Protein Eng. 6 1047–1054.

Wendoloski, J. J.; Matthew, James B.; Weber, P. C.; Salemme, F. R (1987) "Molecular dynamics of a cytochrome c-cytochrome b5 electron transfer complex" Science 238

Whitford, D., Concar, D.W., Veitch, N.C., and Williams, R.J.P. (1990). "The formation of protein complexes between ferricytochtome b5 and ferricytochrome c studied using high-resolution 1H-NMR spectroscopy." Eur. J. Biochem. 192, 715–721.

Willie, A., (1992) "Photoinduced electron transfer in biological systems" Dissertation University of Arkansas, Fayetteville, AR

Willie, A., Stayton, P.S., Sligar, S.G., Durham, B., and Millett, F. (1992). "Genetic engineering of redox donor sites—measurement of intracomplex electron transfer between ruthenium-65 Cytochrome b5 and cytochrome c." Biochemistry 31, 7237–7242.

Yankovskaya V, Horsefield R, Törnroth S, Luna-Chavez C, Miyoshi H, Léger C, Byrne B, Cecchini G, Iwata S, et al. (2003). "Architecture of succinate dehydrogenase and reactive oxygen species generation". Science 299, 700–704

Yinling Zhang (2016) "Two-electron Quenching of Dinuclear Ruthenium (II) Polypyridyl Complexes" Master's Thesis, University of Arkansas, Fayetteville, AR